

Dynamic Analysis of Spine Mechanics

Harriet Violet Chorney

Department of Mechanical Engineering
McGill University, Montreal

August 2023

A thesis submitted to McGill University in partial fulfillment of the
requirements of the degree of Master's of Science

©Harriet Violet Chorney, 2023

Acknowledgements

I would like to first acknowledge my co-supervisors Professor Mark Driscoll and Professor James Forbes for their guidance and mentorship during my tenure at McGill. This work would not have been possible without their direction. Next, I would like to acknowledge the members of the MBR and DECAR groups who helped me along the way and have quickly become some of my closest friends. Specifically, I would like to thank Brittany Stott and Steven Dahdah who have helped me with this work extensively by both guiding me when I was stuck and making sure my writing actually made sense.

In my personal life, I would like to acknowledge my parents Julie Thomson and Chris Chorney, who have encouraged and supported me at every step. I would also like to thank my boyfriend Jackson Empey for always empowering me to reach new heights. Lastly, I would like to thank my friends for being a source of kindness and for providing me with a break whenever I needed it.

Contents

Acknowledgements	ii
Contents	iii
List of Equations	vi
List of Figures	viii
List of Tables	x
List of Abbreviations	xi
Abstract	xiii
Chapter	
1. Introduction	1
2. Literature Review	3
2.1 Spine Anatomy and Physiology	4
2.1.1 Low Back Pain	6
2.1.2 Summary	7
2.2 Surgical Intervention	7
2.2.1 Surgical Simulation	7
2.2.2 Modelling Surgical Movement	9
2.2.2.1 The Frequency Domain	10
2.2.3 Modelling Tissue Force Feedback	11
2.2.3.1 System Identification	14
2.2.4 Summary	15
2.3 Preventative Measures	15
2.3.1 Spine Stability	16
2.3.2 Lyapunov Exponents	18
2.3.3 Basins of Attraction	18
2.3.4 Summary	20

2.4	Conclusion	21
3.	System Identification and Simulation of Soft Tissue Force Feedback in a Spine Surgical Simulator	22
3.1	Framework of Article 1	22
3.2	Article 1: System Identification and Simulation of Soft Tissue Force Feedback in a Spine Surgical Simulator	24
3.2.1	Abstract	24
3.2.2	Introduction	25
3.2.3	Methods	29
3.2.3.1	System Identification	30
3.2.3.2	Simulator Trials	35
3.2.4	Results	36
3.2.4.1	System Identification	36
3.2.4.2	Simulator Trials	39
3.2.5	Discussion	40
3.2.6	Conclusion	43
3.2.7	Acknowledgments	43
3.2.8	References	44
3.2.9	Summary	49
4.	Basin of Attraction Estimate for Analyzing Manual Materials Handling Tasks	51
4.1	Framework of Additional Study	51
4.2	Additional Study: Basin of Attraction Estimate for the Analysis of Manual Materials Handling Tasks	52
4.2.1	Abstract	52
4.2.2	Introduction	52
4.2.3	Methods	55
4.2.3.1	Trajectory Generation	57
4.2.3.2	Feedback Controller	58
4.2.3.3	BOA Computation	59
4.2.4	Results	60
4.2.5	Discussion	63
4.2.6	Conclusion	65
4.2.7	References	65
5.	Discussion	69
5.1	Future Work	73
6.	Conclusion	75

Appendices	77
References	81

List of Equations

2.1	The Fourier series.	10
2.2	The Fourier coefficient for $\cos(kx)$	10
2.3	The Fourier coefficient for $\sin(kx)$	10
2.5	The complex Fourier series.	11
2.6	The discrete Fourier transform.	11
2.7	The least squares cost function.	14
2.9	Solution to the least squares cost function.	15
2.10	Definition of Lyapunov stability.	16
2.11	Definition of Lyapunov asymptotic stability.	16
2.12	Lyapunov's direct method.	19
2.13	Sum of squares polynomial.	19
2.14	Monomial basis vector.	19
2.15	Cholesky factorization of sum of squares polynomial.	19
2.16	Lyapunov parameterization cost function.	20
2.17	Time-varying Lyapunov function.	20
3.1	The Schroeder multisine.	30
3.2	The chirp signal.	30
3.3	The Maxwell model.	31
3.4	The Kelvin Boltzmann model.	32
3.5	The Kelvin-Voigt model.	32
3.6	The autoregressive with exogenous inputs model.	32

3.7	The least squares cost function with Tikhonov regularization.	32
3.8	The solution to the least squares cost function with Tikhonov regularization. . .	33
3.9	A discrete-time transfer function.	33
3.10	The mean residuals.	33
3.11	The fit ratio.	34
3.12	The percent variance accounted for.	34
3.13	The normalized mean squared error.	34
3.14	The matrix condition number.	34
3.15	The relative uncertainty.	34
3.18	The discrete-time state space representation.	35
4.1	The dynamics of a simple pendulum.	56
4.2	The differential Riccati equation.	58
4.3	The time-varying linearization of the dynamics.	58
4.4	The feedback law.	59
4.5	The generalized S-procedure.	59
4.6	The optimization problem for a basin of attraction.	60
4.7	The parameterized Lyapunov function.	60

List of Figures

1.1	Workflow and breakdown of the subsequent chapters of this work.	2
2.1	The spine segmented at the different levels. Depicted from bottom to top: Coccyx, Sacral, Lumbar, Thoracic, and Cervical regions of the spine, obtained from [3].	5
2.2	A vertebral body with an IVD from a lateral and superior view, obtained from [8].	5
2.3	(a) Synthetic benchtop simulator obtained from [35]. (b) Robot-assisted VR simulator obtained from [36].	9
2.4	The autoregressive with exogenous inputs (ARX) model.	14
3.1	Workflow of Article 1	23
3.2	Schematics of tissue force feedback models under consideration from left to right: the Maxwell (MW), the Kelvin Boltzmann (KB), the blackbox higher-order (HO), and the inverted linear (IL) model.	30
3.3	(a) Setup for the system identification experiments with the tool tip for the surgery fixed to the top and the tissue analogue fixed to the bottom and tool tip direction indicated. (b) Experimental setup used by study participants in the simulation that consisted of the game engine, questionnaire, haptic device, tissue analogue, and model test space.	31
3.4	A segment [1, 7] s of the dynamic input (z) and output (<i>Force</i>) signals obtained from the system identification experiments. (a) Chirp, (b) Gaussian noise, (c) Shroeder multisine.	37

3.5	A segment of multisine data from the tissue force response between [1, 7] s compared to the corresponding output from the Maxwell (MW), Kelvin Boltzmann (KB), and higher-order (HO) models.	38
4.1	The inverted pendulum model of the total body center of mass for flexion/extension. Figure modified from [18].	56
4.2	The markers on the torso and their corresponding segments: thorax, abdomen, and pelvis. Figure modified from [20].	57
4.3	Finite-time horizon LQR solution with expanded BOA over the abdomen COM trajectory projected onto $\theta, \dot{\theta}$	61
4.4	BOA around trajectories of each COM of an expert lifter: thorax, abdomen, pelvis. BOAs are projected onto the $\theta, \dot{\theta}$ region of state space. Figure modified from [20]	62
A.1	Ethics approval for work in Chapter 3	79
A.2	Ethics approval for work in Chapter 4	80

List of Tables

2.1	A summary of mass-spring-damper models used to model tissue force feedback. The table includes the name of the model, a depiction of its mechanical analogue, the corresponding force equation, any definitions of parameters, and corresponding references, where $x(t)$ represents position and $f_e(t)$ represents force.	13
2.2	The mechanical and clinical definitions of spine stability.	17
3.1	Error metrics obtained during the exhaustive search for the MW, KB and HO models. The metrics obtained were: the condition number the percent variance accounted for (%VAF), the maximum relative uncertainty of the parameters (MRU), the FIT ratio, the mean residuals, the normalized mean squared error for the testing and training data and the ridge regression coefficient (alpha).	38
3.2	On the left side are the descriptive statistics of the Likert scale data as well as the percentage of participants ($N = 45$) who selected that model as the best performing once completing the experiment. On the right are the p-values from the Mann-Whitney U-test between the model ratings from study participants.	39
4.1	Percent difference in average cross-sectional area of the basin of attraction for each COM, in the depositing task, between an expert and novice, and for a decrease in mass (DM) from 23 kg to 15 kg	63
5.1	Objectives addressed in this thesis. The manuscript explored modelling of spine soft tissue force feedback while the additional study modelled trunk stability along a trajectory.	71

List of Abbreviations

LBP	Low Back Pain
LIF	Lumbar Interbody Fusion
IVD	Intervertebral Disk
MI	Minimally Invasive
VR	Virtual Reality
DFT	Discrete Fourier Transform
FEM	Finite Element Method
ID	Identification
ARX	Autoregressive with Exogenous Inputs
EP	Equilibrium Point
SOS	Sum of Squares
BOA	Basin of Attraction
KB	Kelvin-Boltzmann
HO	Higher-Order
%VAF	Percent Variance Accounted for
MW	Maxwell
KV	Kelvin-Voigt

IL	Inverted Linear
FIT	Fit Ratio
NMSE	Normalized Mean Squared Error
MRU	Maximum Relative Uncertainty
MTS	Material Testing System
MMH	Manual Materials Handling
COM	Centre of Mass
LQR	Linear Quadratic Regulator
DRE	Differential Riccati Equation
aCSA	Average Cross-Sectional Area
MSD	Mass-Spring-Damper

Abstract

This thesis focuses on utilizing concepts from control systems engineering to provide additional insight into approaches for low back pain (LBP) care, specifically considering surgical intervention and preventative measures. LBP is a leading cause of disability and imposes economic strain on the healthcare system. Despite its high prevalence, the cause of many LBP cases remain unknown.

Surgical intervention is often required when preventative measures do not alleviate LBP. One method used to train and improve a surgeon's operational skills is through surgical simulation. In this thesis, a lumbar interbody fusion simulator was studied, with a focus on developing dynamic soft tissue models. Force feedback models were built using system identification with dynamic input signals, and evaluated by clinicians using a haptic force feedback device. It was found that the closer the dynamic models matched the signals the more they were favoured by the clinicians. These results carry potential implications for integrating tissue dynamics into soft tissue force feedback models.

Understanding preventative measures to alleviate LBP or reduce the risks of developing pain is important to avoid more invasive interventions. Spinal stability is known to contribute to a healthy spine, and as such, understanding potential factors which may improve spinal stability could be beneficial. A basin of attraction (BOA) was calculated for a single novice and a single expert. The BOAs represent how much an individual can be perturbed along their trajectory while maintaining stability, identified with respect to a target trajectory. The BOAs showed differences in their mean cross sectional areas between lifters, with the novice having smaller BOAs than the expert. Additionally, the novice lifter was more susceptible

to changes in mass of the box they were lifting. These preliminary results indicate that the novice lifter selected trajectories that make them more susceptible to perturbations than the expert lifter, however, further work is needed to demonstrate statistical significance.

Overall, the works presented herein may provide insight to clinical interventions when focused on improving spine health. This thesis demonstrated how systems and control engineering can be leveraged to analyze behaviours that are not easily observed from sensors alone. Techniques such as dynamic modelling and numerical computing provide insight from data into the unseen behaviour of the spine and its musculature.

Résumé

Cette thèse se concentre sur l'utilisation des concepts de l'ingénierie du contrôle pour fournir un aperçu supplémentaire des approches de soins de la lombalgie, en tenant compte spécifiquement de l'intervention chirurgicale et des mesures préventives. La lombalgie est l'une des principales causes d'invalidité et impose une pression économique sur le système de santé. Malgré sa prévalence élevée, la cause de nombreux cas de lombalgie reste inconnue.

Une intervention chirurgicale est souvent nécessaire lorsque les mesures préventives ne soulagent pas la lombalgie. Une méthode utilisée pour former et améliorer les compétences opérationnelles d'un chirurgien est la simulation chirurgicale. Dans cette thèse, un simulateur de fusion intersomatique lombaire a été étudié, en mettant l'accent sur le développement de modèles dynamiques de tissus mous. Des modèles de retour de force ont été construits à l'aide de l'identification du système avec des signaux d'entrée dynamiques et évalués par des cliniciens à l'aide d'un dispositif de retour de force haptique. Il a été constaté que plus les modèles dynamiques correspondaient aux signaux, plus ils étaient favorisés par les cliniciens. Ces résultats ont des implications potentielles pour l'intégration de la dynamique des tissus dans les modèles de retour de force des tissus mous.

Comprendre les mesures préventives pour soulager la lombalgie ou réduire les risques de la développer est important pour éviter les interventions plus invasives. La stabilité vertébrale est connue pour contribuer à une colonne vertébrale saine et, à ce titre, la compréhension des facteurs potentiels susceptibles d'améliorer la stabilité vertébrale pourrait être bénéfique. Un bassin d'attraction (BOA) a été calculé pour deux sujets dont le travail nécessite de soulever des objets lourds. Un des sujets est un novice et l'autre est un expert. Les BOA

représentent à quel point un individu peut être perturbé le long de sa trajectoire tout en maintenant une stabilité, identifiée par rapport à une trajectoire cible. Les BOA ont montré des différences dans leurs sections transversales moyennes entre les sujets, le novice ayant des BOA plus petits que l'expert. De plus, le sujet novice était plus sensible aux changements de masse de la boîte qu'il soulevait. Ces résultats préliminaires indiquent que le sujet novice a sélectionné des trajectoires qui le rend plus sensible aux perturbations que le sujet expert, cependant, des travaux supplémentaires sont nécessaires pour démontrer la signification statistique.

Dans l'ensemble, les travaux présentés ici peuvent donner un aperçu des interventions cliniques lorsqu'elles sont axées sur l'amélioration de la santé de la colonne vertébrale. Cette thèse a démontré comment l'ingénierie des systèmes et du contrôle peut être exploitée pour analyser des comportements qui ne sont pas facilement observables à partir de capteurs seuls. Des techniques telles que la modélisation dynamique et le calcul numérique fournissent un aperçu des données sur le comportement invisible de la colonne vertébrale et de sa musculature.

Chapter 1

Introduction

The idea that “form implies function” is a heuristic commonly used in human biomechanics since the human form has been built through evolution to fit its environment. This phenomena can be observed in many structures throughout the body. For example, the orientation of the fibers in bone can indicate the direction that bone is loaded in. The ability to identify such mechanisms that allow the human body to function is imperative for scientific understanding and effective clinical intervention.

The spine is a critical structure in the human body that provides mobility and support. The spine works in multiple degrees of freedom and is a high-dimensional nonlinear system. As a result, it can be difficult to capture many of its characteristics using solely imaging and raw data obtained from sensors. This thesis leverages techniques from systems and control engineering to determine information from data that would be otherwise inaccessible. The purpose of this work is to improve on the current state of the art for surgical intervention and preventative measures for lower back pain (LBP).

The motivations of this work are addressed using the workflow depicted in Figure 1.1. The corresponding objectives are as follows:

- **Chapter 3:** Develop and evaluate dynamic soft tissue force feedback models to be used for the surgical simulation of a lumbar interbody fusion procedure.
- **Chapter 4:** Develop estimates for a basin of attraction to characterize manual material handling tasks.

The literature review in Chapter 2 motivates these objectives, and the discussion in Chapter 5 reviews how these objectives were addressed and discussed limitations and opportunities for future work.

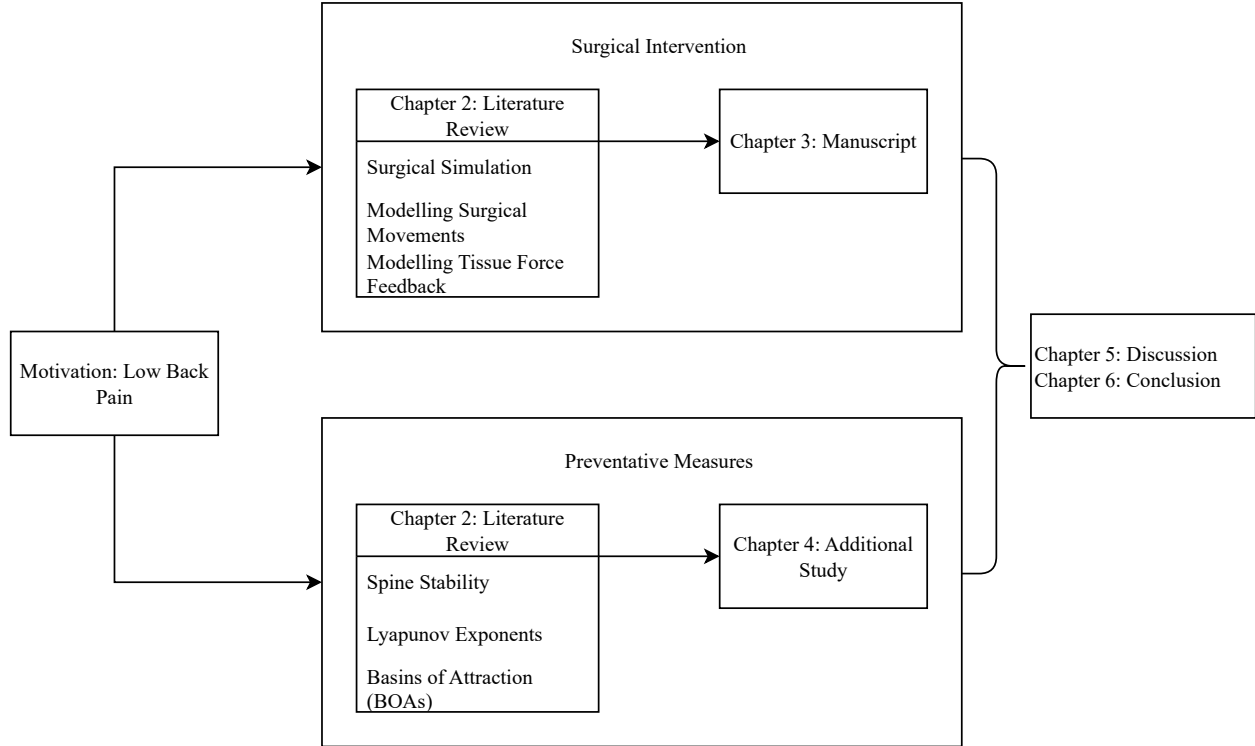


Figure 1.1: Workflow and breakdown of the subsequent chapters of this work.

Chapter 2

Literature Review

The spine has a highly ordered structure, consisting of both passive and active components. It works in tandem with soft tissues and surrounding systems to function. There are multiple anatomical structures and physiological phenomena that contribute to its complex role in the human body and allow it to play an integral part in mobility and support. The development of pathologies in these structures can result in pain that can often require clinical intervention. In this thesis, both surgical interventions and preventative measures to address back pain are explored. For surgical intervention, high-fidelity robot-assisted virtual reality surgical simulators have been developed for training purposes, which require realism for modelling human systems. For preventative measures, techniques to assess spine stability have been developed to characterize tasks that may cause back pain if done incorrectly. The following chapter provides an overview of:

- **Spine Anatomy and Physiology:** this section describes the structure of the spine and mechanisms which contribute to low back pain (LBP).
- **Surgical Intervention:** this section describes surgical simulation of the lumbar interbody fusion (LIF) procedure, and explains the current state of the art for modelling surgeon movement and tissue force feedback to implement in surgical simulators.
- **Preventative Measures:** this section discusses the current state of the art for defining spine stability about a static equilibrium point and along a trajectory to characterize tasks that can cause back pain.

2.1 Spine Anatomy and Physiology

The spine can be broken down into five distinct regions: two sections of fused bones, and three sections demarcated by vertebral bodies along the column. Inferior to the sections of vertebrae are five fused sacral bones that make up the sacrum, and four fused bones that make up the coccyx [1]. The inferior most section of vertebrae consists of five vertebral bodies (L1 - L5), referred to as the Lumbar region of the spine, then twelve thoracic vertebral bodies (T1 - T12), and seven cervical vertebral bodies (C1 - C7) moving superiorly along the column [1]. These segments are summarized in Figure 2.1. Beyond the column, the *global* spine includes intervertebral disks (IVDs), the rib cage, ligaments, and spinal musculature [2]. In particular, the IVDs and spinal musculature play integral roles in spine support and stability, as they help resist the significant loads applied to the spine during everyday activity.

The IVDs are important components in the spine, as issues with the IVDs can be a primary source of back pain and can cause changes in the biomechanics of the spine [4, 5]. The IVDs make up a significant portion of the global spine, contributing to approximately 20 – 33 % of the height of the spine [4]. The two main components of the IVDs are the nucleus pulposus and the anulus fibrosus, as seen in Figure 2.2. The nucleus pulposus is a gelatinous proteoglycan-rich structure with a high water content, which allows large loads to be sustained in the vertebral body [6]. The load is distributed to the collagen-rich anulus fibrosus through hydrostatic pressure [6]. In a healthy individual, the anulus fibrosus has a fiber orientation that allows it to resist the corresponding hoop stress from the nucleus pulposus [6, 7]. These structures allow the IVD to carry large compressive loads while maintaining flexibility in the spine [6].

The muscles appended to the spine are classified as striated skeletal muscles. Contractions are mediated by the nervous system, which send signals at neuromuscular junctions [9]. The spine skeletal muscles attach to the vertebral column through tendons, which are a tissue type that serves to attach muscles to bones in the human body [10]. The muscles play a large role in the ability for the spine to stabilize itself [11]. The ability for humans to stand

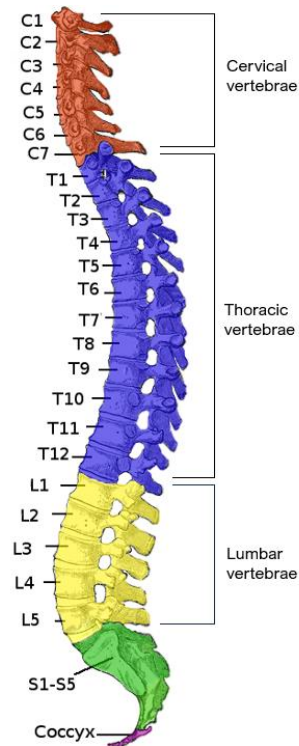


Figure 2.1: The spine segmented at the different levels. Depicted from bottom to top: Coccyx, Sacral, Lumbar, Thoracic, and Cervical regions of the spine, obtained from [3].

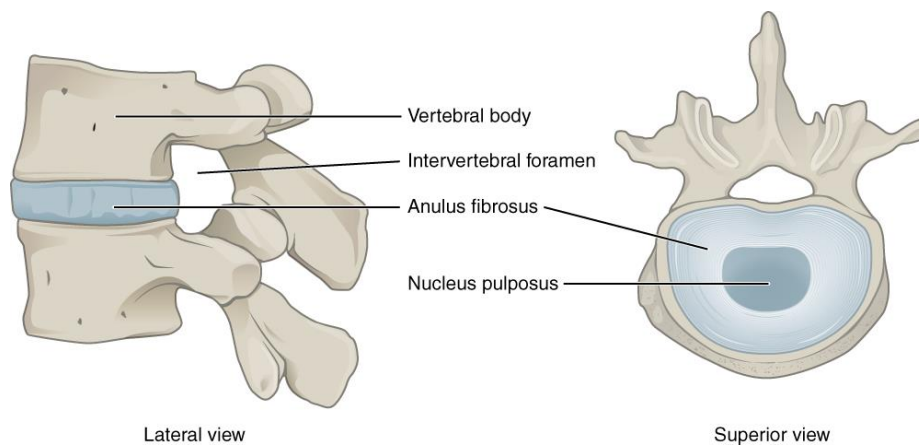


Figure 2.2: A vertebral body with an IVD from a lateral and superior view, obtained from [8].

upright for bipedal motion is largely attributed to a muscle group called the erector spinae [4]. The erector spinae is composed of three muscles: the spinalis, longissimus and iliocostalis [12]. Another large muscle group that is attached to the spine is the psoas major, which extends the upper lumbar spine to help with lifting and flexion [12, 13]. Additionally, the multifidus muscle group aids with producing extension of the vertebral column [4]. In general, these large muscle groups contribute to the overall stability and support along the vertebral column.

As with many biological structures, the shape of the spine informs its function. There is a distinct change in the size and shape moving downward from the cervical region towards the coccyx. This change in shape reflects the load-bearing ability of the vertebral bodies are dependent on its size, shape and density [11]. In particular, the loads from body weight and stresses from muscles increase moving down the spine, with the average strength of the cervical segment and the lumbar segment being 2000 N and 8000 N respectively [11, 14]. These large loads on the lower back can lead to high incidence of low back pain.

2.1.1 Low Back Pain

Low back pain (LBP) is a common health problem, with a lifetime prevalence between 49-70%. LBP is considered a foremost cause for work absence and limitation of activity [15–17]. Clinically, LBP can occur due to mechanical conditions such as a degenerative disc, neurogenic conditions such as spinal stenosis, non-mechanical spinal conditions such as an infection, referred visceral pain such as renal disease, or other causes such as fibromyalgia [18]. Many factors influence an individual’s potential to experience back pain, some are genetic, while others are due to circumstance. For example, occupational weight lifting is associated with a higher incidence of LBP [18, 19]. As such, the ability to prescribe proper lifting techniques is a clinically relevant issue for intervention of LBP [20]. Additionally, degenerative disc disease is the most common cause of LBP and has been attributed to both fatigue from high cyclic loading as well as genetic factors [21]. Degenerative diseases of the

spine can be addressed with surgical intervention [21].

2.1.2 Summary

The spine has an ordered structure that is influenced by the vertebrae, IVDs, and spine musculature. The structure of the spine allows it to take on high loads in daily activities. However, often people experience pain in the lower regions of the spine. LBP is multifactorial and complex as it can be caused both through genetic and environmental factors. In certain cases, environmental factors which cause LBP can be mitigated with clinical intervention. When preventative measures are ineffective, surgery can be performed to alleviate pain.

2.2 Surgical Intervention

Lumbar interbody fusion (LIF) surgeries are used to stabilize a segment of the lumbar spine by fusing two vertebrae [22]. This is usually performed when a patient presents with longterm LBP from degenerative disease of the lumbar spine [23]. LIF is a procedure that navigates the soft tissues in the back to access an IVD and perform a discectomy, which is a removal of the disk [22]. The IVD is then replaced with an implant, typically a cage, spacer, or structural graft to fuse the vertebrae [22]. Certain LIF procedures are classified as minimally invasive (MI) since access to the IVD can be obtained with a laparoscopic probe [24].

2.2.1 Surgical Simulation

Results from a 2019 meta-analysis found that 1 in 20 patients experience harm from preventable errors made during medical treatment [25]. With LIF procedures being a relatively common MI surgery, improving the teaching practices to avoid errors is important [26]. The Halsted method, commonly described as “See One, Do One, Teach One”, is the traditional method for teaching surgery [27]. The Halsted method takes on the following workflow: the surgical residents will first observe a surgical procedure, and then be expected to perform

that procedure, and finally must teach it to other residents [27]. However, the traditional training methods have limitations such as a lack of skill proficiency training and adequate skill assessment [28, 29]. These drawbacks can be addressed using surgical simulation [28, 30].

Surgical simulators take on many forms to help train surgeons at different levels. A surgical simulator is often characterized by its fidelity, indicating how well it can replicate a given surgery [31]. Low-fidelity simulators tend to allow for practicing only a specific, usually basic, surgical skill, whereas high-fidelity simulators are able to realistically emulate the surgery and are better suited to train more advanced surgeons [32]. Surgical simulators can be further sub-categorized as organic and inorganic. Organic simulators typically take the form of operations on live animals or on cadaveric models [31]. Operations on live animals can be effective because they can share many characteristics with operations on humans. However, the anatomical structures of the animals used can vary greatly from human beings [32]. Additionally, there are ethical concerns surrounding their use [31–33]. Cadaveric models are another organic simulator used in surgical simulation and they are commonly regarded as the gold standard due to their proximity to living human tissue [32]. However, cadavers are often too expensive in practice to be used frequently as they also cannot typically be reused following many procedures [32]. It should also be noted that depending on the post-mortem treatment of the cadavers, fidelity in the tissue force feedback can be lost as well [34].

Synthetic simulators that employ polymeric materials and tissue analogues are also common for both high- and low-fidelity simulations. The higher-fidelity analogues, like the one in Figure 2.3a, can accurately recreate complex procedures, particularly in the context of minimally invasive surgery [32, 37]. In certain cases, these models can be 3D-printed and customized to specific patients as a result [34, 38, 39]. Many high-fidelity analogues have been validated for use in surgical skill training activities including obtaining access in laparoscopic surgery and image-guided needle-based interventions [40, 41]. However, the high-fidelity analogues tend to have a higher cost which can make them less accessible as training modalities [32].



(a)



(b)

Figure 2.3: (a) Synthetic benchtop simulator obtained from [35]. (b) Robot-assisted VR simulator obtained from [36].

Virtual reality (VR) simulation is the newest form of surgical simulation, having first been introduced in the 1990s [32]. These inorganic simulators provide the operator with images on a computer that can be manipulated to emulate a given surgery. The robot-assisted VR simulators, like the one in Figure 2.3b, were then introduced soon after the VR simulators in 1999, with the first one being the da Vinci surgical system [32]. Robot-assisted surgical simulators can utilize VR for visual and auditory feedback, and a robotic haptic device to convey the forces experienced during the surgery to the operator [42]. The haptic feedback is particularly important for MI surgical simulation when obtaining access to the target structure (in the LIF procedure, this is when the surgeon gains access to the IVD), as the surgeon relies almost entirely on tactile feedback during this step. As such, adequate models of soft tissue force feedback add realism to LIF surgical simulators, which requires modelling both how the surgeon interacts with the soft tissue and the resulting tissue force response.

2.2.2 Modelling Surgical Movement

Transforming signals measured from a surgeon’s movement to the frequency domain can provide insight into how the surgeon may excite tissue during surgery and quantifies bandwidths that may not be easily observed in the time domain. The frequency domain is exploited in surgical robotics studies for motion compensation of physiological tremors

[43]. This is because the motion of the surgeon while performing the surgery occupies a different bandwidth than their tremors in the frequency domain [43]. This is an example of behaviour that is more easily observed in the frequency domain than in the time domain. The movements made by surgeons are also commonly explored in surgical skill assessment literature. Surgical skill assessment uses artificial intelligence to compartmentalize surgical skill level and augment VR training modalities [30]. Modelling the surgical movement in the frequency domain using a discrete Fourier transform (DFT) has previously provided an excellent classification result [44, 45]. Therefore, modelling a surgeon's movement in the frequency domain can be divided into different bandwidths.

2.2.2.1 The Frequency Domain

The Fourier series provides one method of transforming signals into the frequency domain. Specifically, and periodic, piecewise smooth function $f(x)$ can be represented as

$$f(x) = \frac{a_0}{2} + \sum_{k=1}^{\infty} (a_k \cos(kx) + b_k \sin(kx)), \quad (2.1)$$

where equation (2.1) can be thought of as an infinite sum of sine and cosine functions of increasing frequency [46]. The coefficients a_k and b_k are formally defined as the Hermitian inner products of $f(x)$ and the orthogonal cosine and sine bases $\{\cos(kx), \sin(kx)\}_{k=0}^{\infty}$ [46]. Intuitively, it can be thought of as the projection of $f(x)$ onto $\cos(kx)$ and $\sin(kx)$ [46]. This is analogous to a dot product between two vectors in Euclidean space. As such, the coefficients can be rewritten as

$$a_k = \frac{1}{\|\cos(kx)\|^2} \langle f(x), \cos(kx) \rangle \quad (2.2)$$

and,

$$b_k = \frac{1}{\|\sin(kx)\|^2} \langle f(x), \sin(kx) \rangle. \quad (2.3)$$

Using Euler's formula, $e^{ikx} = \cos(kx) + i\sin(kx)$, the Fourier series can be written in a

complex form,

$$f(x) = \sum_{k=-\infty}^{\infty} (\alpha_k + i\beta_k)(\cos(kx) + i\sin(kx)) \quad (2.4)$$

$$= \sum_{k=-\infty}^{\infty} c_k e^{ikx}. \quad (2.5)$$

The Fourier series applies to periodic functions but is often needed for nonperiodic functions as well. The Fourier transform allows the Fourier series to approximate functions that are not necessarily periodic. The Fourier transform is derived by defining the Fourier series on the domain $x \in [-L, L)$ and taking the limit $L \rightarrow \infty$ [46]. This ultimately results in the Fourier transform pair that converges on a solution [46]. The practical implementation is the DFT because it allows the Fourier analysis to be performed on numerically on a computer [46]. The DFT takes the form of a linear system of equations, $\mathbf{Ax} = \mathbf{b}$, with a linear operator that maps data points in the time domain f into the frequency domain \hat{f} [46]. The linear transformation is defined as a unitary Vandermonde matrix to formulate the DFT [46]

$$\begin{bmatrix} \hat{f}_0 \\ \hat{f}_1 \\ \hat{f}_2 \\ \vdots \\ \hat{f}_{N-1} \end{bmatrix} = \begin{bmatrix} 1 & 1 & 1 & \dots & 1 \\ 1 & \omega_N^{-1} & \omega_N^{-2} & \dots & \omega_N^{-(N-1)} \\ 1 & \omega_N^{-2} & \omega_N^{-4} & \dots & \omega_N^{-2(N-1)} \\ \vdots & \vdots & \vdots & & \vdots \\ 1 & \omega_N^{-(N-1)} & \omega_N^{-2(N-1)} & \dots & \omega_N^{-(N-1)^2} \end{bmatrix} \begin{bmatrix} f_0 \\ f_1 \\ f_2 \\ \vdots \\ f_{N-1} \end{bmatrix}. \quad (2.6)$$


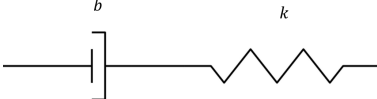
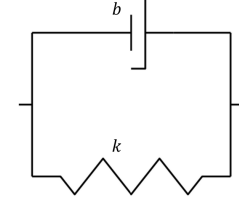
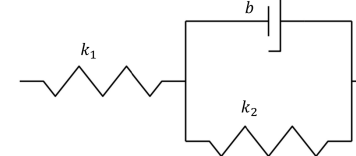
2.2.3 Modelling Tissue Force Feedback

Tissue force feedback models have been generated in many different ways for surgical simulation and surgical robotics. One common way is through the use of the finite element method (FEM), in which the tissue deformation is modelled as a spatial discretization of the continuum mechanics of the materials [47]. This method is often criticized for its computational complexity in the context of surgical simulation, as haptic feedback requires a 100 ms computation time, necessitating efficient modelling techniques [48, 49]. To address time

restrictions, kinematic and dynamic models have been developed for tool-tissue interaction [50, 51]. For example, modelling needle bending for force feedback of needle insertion has been done using beam models [52]. These models are meshless and often exploit very complex dynamics that must be determined through rigorous experimental testing [49, 52]. Additionally, these models are typically not transferable to other systems, with the dynamics changing between different tool tips and tissue types [53].

Data-driven approaches such as machine learning have also been used for tissue force feedback modelling. However, these models have been built to replicate an FEM structure or are more suited to surgical robotics applications because they employ vision-based strategies that do not work when the real environment is abstracted to a simulation [54, 55]. Additionally, these approaches are limited to the information obtained from training data, and utilizing models from first principles may be more scalable to applications not previously captured with data. Other studies have fit parabolic curves to measurements from cadavers to find the corresponding force feedback [56]. However, this risks over-fitting to specific cadavers instead of using known tissue behaviour to infer a generalizable model. Tissue viscoelastic models can be exploited to build force feedback models from data. Employing viscoelastic tissue models as a means of modelling force contact between the tool and tissue has been widely applied in the context of surgical robotics [48, 57–59]. A summary of the viscoelastic models employed in literature is in Table 2.1. These models can be most effectively built through a process known as system identification [60].

Table 2.1: A summary of mass-spring-damper models used to model tissue force feedback. The table includes the name of the model, a depiction of its mechanical analogue, the corresponding force equation, any definitions of parameters, and corresponding references, where $x(t)$ represents position and $f_e(t)$ represents force.

Name	Mechanical Analogue	Equation	Parameter Definition	Ref.
Linear Elastic		$f_e(t) = kx(t)$	-	[48, 57]
Maxwell		$f_e(t) = b\dot{x}(t) - \alpha f_e(t)$	$\alpha = b/k$	[48, 57]
Kelvin Voigt		$f_e(t) = kx(t) + b\dot{x}(t)$	-	[48, 57–59]
Kelvin Boltzmann		$f_e(t) = kx(t) + \nu\dot{x}(t) - \gamma\dot{f}_e(t)$	$k = k_1k_2/(k_1 + k_2)$ $\nu = bk_2/(k_1 + k_2)$ $\gamma = b/(k_1 + k_2)$	[48, 57]

2.2.3.1 System Identification

System identification (ID) is a modelling approach that can both be data-driven and exploit known system mechanics [60]. In general, system ID uses input and output data to inform a model, which is what categorizes it as data-driven [60]. However, system ID can be further sub-classified as grey-box modelling and black-box modelling, also called parametric and non-parametric modelling [60]. When doing grey-box (or parametric) modelling, data is fit to a pre-determined model structure, which is what allows system ID to exploit known system mechanics [60]. Black-box (or non-parametric) modelling uses only the data to inform a model structure as well as how that model is parameterized.

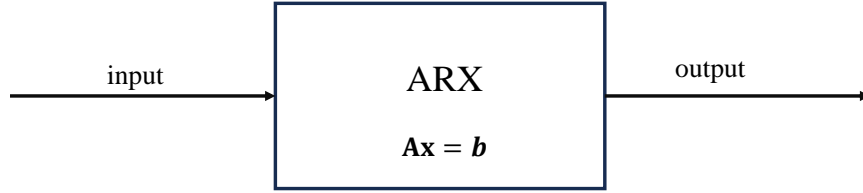


Figure 2.4: The autoregressive with exogenous inputs (ARX) model.

The equation $\mathbf{Ax} = \mathbf{b}$ represents a problem with known data matrices \mathbf{A} and \mathbf{b} , while \mathbf{x} contains unknown parameters. In particular, this is the formulation for an autoregressive with exogenous inputs (ARX) model, shown in Figure 2.4. The ARX model can be solved with a least squares approach [61, 62]. The objective is to minimize the cost function

$$J(\mathbf{x}) = \frac{1}{2} \|\mathbf{Ax} - \mathbf{b}\|_2^2, \quad (2.7)$$

where $\|\cdot\|_2$ denotes the Euclidean norm. Differentiating $J(\mathbf{x})$ with respect to \mathbf{x} and setting it to zero gives

$$\mathbf{A}^\top \mathbf{Ax} = \mathbf{A}^\top \mathbf{b}. \quad (2.8)$$

The parameters can then be approximated as

$$\hat{\mathbf{x}} = (\mathbf{A}^\top \mathbf{A})^{-1} \mathbf{A}^\top \mathbf{b}. \quad (2.9)$$

The input data contained in \mathbf{A} , should be sufficiently varying to ensure that the matrix is full column rank, so that $\mathbf{A}^\top \mathbf{A}$ is positive definite and the solution $\hat{\mathbf{x}}$ is a unique minimizing solution. The data is typically normalized or standardized during the system identification procedure to account for differences in units amongst parameters. The technique of system identification has been widely used in various applications, such as for identifying models for flight simulators and for identifying physiological systems [62–64]. Additionally, ARX models have been previously used to model tissue behaviour for biomedical applications [65, 66].

2.2.4 Summary

Surgical simulation provides a valuable resource and training modality for surgeons. The minimally invasive LIF procedure necessitates a high fidelity simulation. In particular, gaining access to the IVD during this procedure requires realistic tissue force feedback models, which necessitates accurate modelling of the interaction between the surgeon and tissue. Modelling the surgeon can be done by utilizing the frequency domain because surgeon movements during an operation are within a bandwidth of frequencies. Modelling soft tissue can then be developed by exploiting tissue properties and using data-driven techniques such as system ID in the bandwidth of frequencies of the surgeon.

2.3 Preventative Measures

One way to prevent LBP is by mitigating environmental factors. For example, being able to characterize incorrect lifting techniques, which is associated with high incidence of LBP [18, 19]. Systems, such as the spine during lifting, can be fundamentally characterized through stability. The stability of the spinal column is critical for movement, bearing loads, and avoiding pain [67]. Unlike other autonomous systems such as drones or manipulator

arms, many systems in the human body are not observable through sensors [68]. Previously inaccessible signals and systems in the spine can be more readily estimated by leveraging systems and control theory [68–71]. Understanding stability can also potentially provide clinical insight into pathological mechanisms underlying pain [68].

2.3.1 Spine Stability

The spine on its own is an inherently unstable system. However, in tandem with other structures in the body, the spine becomes stable. The vertebrae, discs, and ligaments constitute the passive components, while the muscles and tendons can be considered active, and the surrounding neurological system acts as a transducer to direct the active components [72]. Problems arising in these subsystems could hinder spine stability and lead to pain and sub-optimal adaptations to compensate for abnormal behaviour [67, 72–74]. There is little consensus on a definition of spine stability. Generally, the definitions can be subdivided into two groups: the mechanical definition and the clinical definitions in Table 2.2. The mechanical definition of stability closely aligns with the Lyapunov definition about an equilibrium point (EP) [68]. The EP defined as $\bar{\mathbf{x}} = \mathbf{0}$ of the system $\dot{\mathbf{x}}(t) = \mathbf{f}(\mathbf{x}(t))$, with the initial conditions $\mathbf{x}(0) = \mathbf{x}_0$, is considered Lyapunov stable if $\forall \epsilon > 0, \exists \delta(\epsilon) > 0$ such that

$$\|\mathbf{x}_0\| < \delta(\epsilon) \Rightarrow \|\phi(t, \mathbf{x}_0)\| < \epsilon, \quad \forall t \geq 0. \quad (2.10)$$

The system is considered locally asymptotically stable if it is Lyapunov stable and $\exists \eta > 0$ such that [78]

$$\|\mathbf{x}_0\| < \eta \Rightarrow \lim_{t \rightarrow \infty} \|\phi(t, \mathbf{x}_0)\| = 0. \quad (2.11)$$

If neither conditions are met then the system is considered unstable about that EP [78]. Roughly speaking, this means that after an impulse, the system is Lyapunov stable when the system’s trajectory stays within a region of the EP, and it is considered asymptotically stable when it is Lyapunov stable and converges to the EP [78]. In the context of spine stability,

Table 2.2: The mechanical and clinical definitions of spine stability.

Type	Defintion	Ref
Mechanical Definition	<p><i>“we must give a small perturbation and observe the new behavior. If the new behavior is approximately the same as the old, qualitatively speaking, the system is stable. If the changed behavior becomes indistinguishable from the old behavior, returning to its original position or trajectory after a sufficiently long time, the system is asymptotically stable. Finally, if the disturbed behavior differs significantly from the old behavior, the system is unstable.”</i></p>	[75]
Clinical Definition	<p><i>“the ability of the spine to limit its patterns of displacement under physiologic loads so as not to damage or irritate the spinal cord or nerve roots”</i></p>	[76]
	<p><i>“the capacity of the vertebrae to remain cohesive and to preserve the normal displacements in all physiological body movements”</i></p>	[77]

the mechanical definition is criticized for being more suited to quantifying stability about an EP, as opposed to quantifying stability about a trajectory [67, 79]. Mechanical stability of the spine can be considered “static” when it is about a static EP, but when the EP is time-dependent such as along a trajectory, then it is considered “dynamic” stability [67, 79]. Additionally, different components of the body contribute to static and dynamic stability. In static stability baseline intra-abdominal pressure has played a larger role by increasing stiffness in the abdominal cavity [80]. While in dynamic stability, time-varying properties of tissue, neuromuscular control, and time-dependent reflex-responses are the main contributing factors [77, 81]. Human beings are often moving beyond a single point, leading to effects from kinetic energy or inertia that cannot be captured by a static equilibrium [79].

2.3.2 Lyapunov Exponents

One way that spine stability along a trajectory is quantified in literature is through the use of Lyapunov exponents. In nonlinear systems theory, Lyapunov exponents have been used to quantify how sensitive the system is to a set of initial conditions [79, 82]. Considering the initial conditions of the trajectory as a sphere, as time progresses and the system moves along the trajectory, the variations in the mechanics cause the sphere to expand and contract in different directions [79, 82]. This leads the sphere to transform into ellipsoids of different shapes over time [79, 82]. The principle axes of these ellipsoids are the Lyapunov exponents [79, 82]. The more negative the Lyapunov exponent, the more the ellipsoids contract, such that the system is converging to the trajectory over time [79, 82]. The more positive the Lyapunov exponents, the more the ellipsoids expand, indicating that trajectories diverge [79, 82]. A system is therefore considered stable when the sum of its Lyapunov exponents is negative [79, 82].

During a repetitive trunk movement, the trajectory kinematics should be similar at each repetition [79]. The variances in repeated trajectories can be attributed to random disturbances and control errors in the movement process [79]. The purpose of Lyapunov exponents in this context is to model neuromuscular responses that keep the trajectories consistent, attracting the trunk's inherent dynamics towards a single trajectory at every repetition of the movement [79]. This can be found by modelling the maximum Lyapunov exponent of nearest neighbors in repeated trajectories [79]. The benefit is that no model of the system is necessary, so the results can be inferred from only data [79]. The use of Lyapunov exponents as a measure of dynamic spine stability has been used for unloaded trunk movements and lifting [67, 83, 84].

2.3.3 Basins of Attraction

Lyapunov's direct method can also be used to evaluate a system's stability. Consider the case of a single EP $\bar{\mathbf{x}} = \mathbf{0}$ [78]. The EP is locally asymptotically stable if there exists *any*

continuously differentiable locally positive definite function $V : \mathbb{R}^n \times \mathbb{R}^+ \rightarrow \mathbb{R}$, where $\mathbf{0} \in D$, such that [78]

$$\begin{aligned} V(\mathbf{0}) &= 0, \\ V(\mathbf{x}(t)) &> 0, \quad \forall \mathbf{x} \in D \setminus \mathbf{0}, \\ \dot{V}(\mathbf{x}(t)) &< 0, \quad \forall \mathbf{x} \in D \setminus \mathbf{0}. \end{aligned} \tag{2.12}$$

These Lyapunov functions can be analogous to energy, and by finding a Lyapunov function candidate that satisfies these conditions it implies that the system converges towards the EP, similar to how energy dissipates. These Lyapunov function candidates can be searched through for a given closed loop system to demonstrate local asymptotic stability about an EP [85]. One way to do so is by using sum of squares (SOS) programming [85]. SOS programming can be used to systematically find Lyapunov functions by parameterizing them as SOS polynomials. A polynomial $p(x)$ with an even-numbered degree can be searched for as SOS *iff* there exists a positive semidefinite matrix \mathbf{Q} that parameterizes a monomial basis vector \mathbf{b} as

$$p(x) = \mathbf{b}^T \mathbf{Q} \mathbf{b}. \tag{2.13}$$

This form expands out to a polynomial function [85, 86]. The monomial basis vector in this case takes on the form of

$$\mathbf{b} = [1 \ x_1 \ x_2 \ \dots \ x_n \ x_1^2 \ x_2^2 \ \dots \ x_n^d]^T. \tag{2.14}$$

If \mathbf{Q} is symmetric positive semidefinite, then \mathbf{Q} can be written as $\mathbf{Q} = \mathbf{A}^T \mathbf{A}$. The SOS polynomial can then expand out to [85, 86]

$$p(x) = \mathbf{b}^T \mathbf{A}^T \mathbf{A} \mathbf{b} = (\mathbf{A} \mathbf{b})^T (\mathbf{A} \mathbf{b}) = \|\mathbf{A} \mathbf{b}\|^2. \tag{2.15}$$

Equation (2.15) is an algebraic certificate of nonnegativity that can be solved for as a semidefinite program using numerical computing software [85, 86]. Therefore, a polynomial

Lyapunov function can be found with the following feasibility problem [87]

$$\begin{aligned}
& \min_{V(\mathbf{x})} -\gamma \\
& \text{s.t. } V(\mathbf{x}) \text{ is SOS} \\
& \quad -\frac{\partial V(\mathbf{x})}{\partial \mathbf{x}} \mathbf{f}(\mathbf{x}) \text{ is SOS.}
\end{aligned} \tag{2.16}$$

Where γ is a slack variable for the feasibility problem, $\mathbf{f}(\mathbf{x})$ is the nonlinear closed loop dynamics approximated as a polynomial, and $\frac{\partial V(\mathbf{x})}{\partial \mathbf{x}}$ is the gradient of the Lyapunov function. This constrains the polynomial Lyapunov function to the conditions in equation (2.12).

A Lyapunov function that satisfies equation (2.12) approximates the invariant set around the EP [88, 89]. An invariant set, \mathcal{G} , can be defined as $\mathbf{x}(0) \in \mathcal{G} \Rightarrow \forall t > 0, \mathbf{x}(t) \in \mathcal{G}$ [88]. This means that once the state enters \mathcal{G} , it stays within the set [88]. A region of attraction is a bounded invariant set that can be approximated with the sub-level invariant sets of Lyapunov functions [90–92]. These sets can be extended along a trajectory to form a basin of attraction (BOA) by adding a time dependency to the Lyapunov function

$$\dot{V}(\mathbf{x}(t), t) = \frac{\partial V(\mathbf{x}(t), t)}{\partial t} + \frac{\partial V(\mathbf{x}(t), t)}{\partial \mathbf{x}} \mathbf{f}(\mathbf{x}(t), t). \tag{2.17}$$

In biomechanics, the use of BOAs has been validated for a sit-to-stand task by using a pendulum as the plant model about a person’s centre of mass (COM) [93, 94]. The inverted pendulum model has been used for the unstable seated balance task to quantify spine stability about an EP as well [95, 96]. Intuitively, the BOA represents the boundaries for which the plant can be perturbed and still converge to the goal set at the end of the trajectory. The optimization problem for the BOA provides a certificate for a bounded invariant set at each point along the trajectory to the goal set.

2.3.4 Summary

Adequately characterizing the stability of the spine can provide insight into how it performs movement, bears loads, and avoids pain. Spine stability has multiple definitions, with the

mechanical definition most closely aligning with the Lyapunov definition of stability. The definitions of stability can extend beyond a static EP to understand how the spine moves along a trajectory. This has been quantified for various tasks using Lyapunov exponents. However, this can also be characterized using BOAs, which have been validated for other mechanical tasks.

2.4 Conclusion

In this work, both surgical interventions and preventative measures are addressed to improve outcomes of LBP using systems and control engineering. Surgical interventions can be addressed by improving training modalities for LIF procedures using robot-assisted VR surgical simulators. Additionally, preventative measures can be addressed by defining spine stability along a trajectory for lifting techniques during manual materials handling tasks. The subsequent chapters examine these topics in a manuscript and an additional study respectively.

Chapter 3

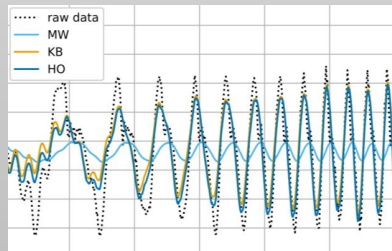
System Identification and Simulation of Soft Tissue Force Feedback in a Spine Surgical Simulator

3.1 Framework of Article 1

The following study exploits the dynamic nature of the soft tissues of the spine to develop force feedback models that were implemented in the haptic device of a surgical simulator. A frequency analysis of surgeon movement was used to generate signals that excite the soft tissue across a bandwidth of frequencies. Subsequently, linear system identification was performed to identify the tissue force feedback behaviour realized as ordinary difference equations. The models were then programmed into a surgical simulator and tested with clinicians. The workflow of the article is depicted in Figure 3.1. Ethics approval was obtained for this study from necessary review boards (see Appendix A). The manuscript was accepted for publication in *Computers in Biology and Medicine* (DOI: <https://doi.org/10.1016/j.compbimed.2023.107267>) [1].

System Identification and Simulation of Soft Tissue Force Feedback in a Spine Surgical Simulator

Results:

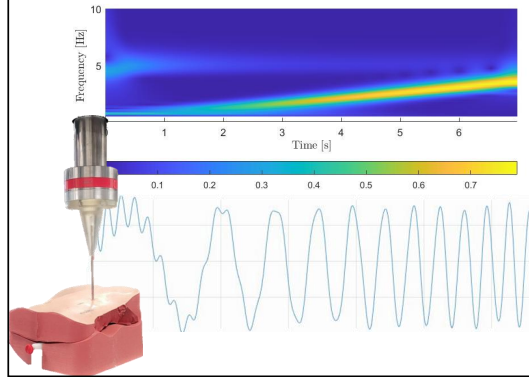


The most accurate model was the highest rated in simulation

Conclusion: This study highlights the importance of utilizing dynamic signals to generate dynamic models of soft tissue for spine surgical simulators

1

Signals: build signals that excite the tissue across a surgeon's frequency bandwidth



3

Simulation: test models in a surgical simulator

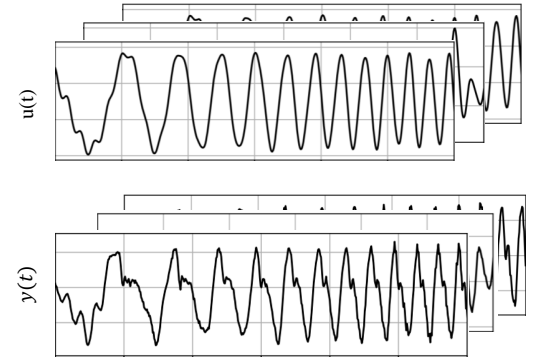
$$\mathbf{x}_k = \mathbf{A}\mathbf{x}_{k-1} + \mathbf{B}u_{k-1},$$

$$y_k = \mathbf{C}\mathbf{x}_k + \mathbf{D}u_k.$$



2

Systems: identify the system as dynamic viscoelastic models



$$\begin{bmatrix} y_N \\ y_{N-1} \\ \vdots \\ y_{n+1} \\ y_n \end{bmatrix} = \begin{bmatrix} -y_{N-1} \dots -y_{N-n} & u_{N-n+m} \dots u_{N-n} \\ -y_{N-2} \dots -y_{N-n-1} & u_{N-n-1+m} \dots u_{N-n-1} \\ \vdots & \vdots \\ -y_n \dots -y_1 & u_{1+m} \dots u_1 \\ -y_{n-1} \dots -y_0 & u_m \dots u_0 \end{bmatrix} \begin{bmatrix} b_{n-1} \\ \vdots \\ b_0 \\ a_m \\ \vdots \\ a_0 \end{bmatrix}$$

$\underbrace{\quad}_{\mathbf{b}} \quad \underbrace{\quad}_{\mathbf{A}} \quad \underbrace{\quad}_{\mathbf{x}}$

$$\min_x \|\mathbf{Ax} - \mathbf{b}\|_2^2 + \|\Gamma\mathbf{x}\|_2^2$$

Figure 3.1: Workflow of Article 1

3.2 Article 1: System Identification and Simulation of Soft Tissue Force Feedback in a Spine Surgical Simulator

Harriet Violet Chorney^{a, b, c}, James Richard Forbes^c, Mark Driscoll^{a, b}

a. The Musculoskeletal Biomechanics Research (MBR) Lab, Department of Mechanical Engineering, McGill University, Montreal, Quebec, Canada

b. Orthopaedic Research Laboratory (ORL), Research Institute MUHC, Montreal General Hospital, Montreal, Quebec, Canada

c. The Dynamics, Estimation, and Control in Aerospace and Robotics (DECAR) Group, Department of Mechanical Engineering, McGill University, Montreal, Quebec, Canada.

Status: Published. DOI <https://doi.org/10.1016/j.compbio.2023.107267>

Corresponding Author: Mark Driscoll email: mark.driscoll@mcgill.ca, phone: 514-398-6299, fax: 514-398-7365

3.2.1 Abstract

Surgical simulators are being introduced as training modalities for surgeons. This paper aims to evaluate dynamic models used to convey force feedback from puncturing the soft tissue during a spine surgical simulation. The force feedback of the tissue is treated as a dynamic system. This is done by performing classical system identification across a bandwidth of frequencies on a tissue analogue and fitting that behaviour to dynamic viscoelastic models. The models that are tested are an inverted linear model, the Maxwell model, the Kelvin-Boltzmann (KB) model, and a higher-order blackbox (HO) model. Several error metrics such as percent variance accounted for (%VAF) are determined to measure solution accuracy. The force feedback models are programmed into a surgical simulator and tested with study participants who rated them based on how well the identified models match the behaviour of the rubber tissue analogue. The highest %VAF is **82.64%** when the tissue is modelled as the HO model. Statistically significant differences ($p < 0.05$) are found between all model

ratings from participants except between the HO model and the KB model. However, the HO model has the highest percentage (**37.8%**) of participants who rank its performance as the closest to the tissue analogue compared to the other force feedback models. The more accurately the dynamic behaviour resembles the tissue analogue, the higher the model was rated by study participants. This study highlights the importance of utilizing dynamic signals to generate dynamic models of soft tissue for spine surgical simulators.

Keywords: System identification, surgical simulation, force feedback, modelling, viscoelasticity

3.2.2 Introduction

The traditional approach for teaching surgery has relied on the Halsted method, commonly described as “See One, Do One, Teach One”, in which a novice surgeon will observe a surgical procedure, and then be expected to perform that procedure, and finally teach it [2]. However, the traditional training methods have limitations that can be addressed with modern technologies to improve surgical training and reduce costs [3, 4]. In particular, surgical simulators are being introduced as training modalities to assess surgical skill level and to impart skill proficiency through repetition without risking harm to a patient, or utilizing high-cost options such as cadavers [5].

Previous surgical simulators have employed physical benchtop models using a tissue analogue made of 3D printed materials or rubber as these are inexpensive non-cadaveric educational models that can mimic tissue characteristics [6]. These benchtop analogues have been validated for use in surgical skill training activities such as obtaining access in laparoscopic surgery and for image-guided needle-based interventions [7, 8]. Other surgical simulators have used virtual reality for visual and auditory feedback with a haptic device to provide force feedback to its operator [9]. One area of interest with respect to these simulators is the force feedback used to simulate the response from soft tissues during surgery. These force profiles add realism and fidelity to the simulators, and have been found to show

particular importance when simulating the access-gaining step during minimally invasive (MI) surgeries [10]. This step varies between different surgical procedures. One methodology is to insert a small probe into a patient through an incision to gain tactile access to the target structure and expand the incision for visual access for the remainder of the surgery [11]. This is the first step of the MI spine interbody-fusion surgery under consideration in this work [11, 12]. Haptic feedback is important during the access-gaining step because the surgeon can rely almost entirely on somatosensory feedback when first puncturing the patient. As such, the models used to generate this force response are important and a pertinent area of study.

Human soft tissue possesses the property of viscoelasticity, and its manipulation over time can be considered a dynamic system as a result [13]. There are multiple ways to model dynamic biomechanical systems. One approach is to derive the behavior of the system from first principles, with parameters determined from experiments [14]. Another approach is data-driven modelling where the system is modelled by the way it transforms a given input dataset to provide a given output dataset, similar to the modelling approaches that have been employed in machine learning [15]. Classical system identification is a data-driven modelling approach that can also exploit known system mechanics from first principles when determining a system model [16]. Linear systems are of particular interest in classical system identification as they can be easily integrated into many modern control systems. Linear systems are formulated as the next output value that is predicted by a linear transformation of a time window of input and output data-points at previous time-steps [16]. System identification has previously been used for modelling in simulation, such as in flight simulators, as well as for identifying multiple dynamic physiological systems [17, 18].

Literature on system identification of tissue force response for haptic feedback has been largely concentrated in the field of surgical robotics [19–22]. Considering the viscoelastic nature of tissue, it is common for researchers to model its force response as mass-spring-damper systems. The most recurrent linear viscoelastic models in these works are: the Maxwell (MW) model, the Kelvin-Voigt (KV) model, and the Kelvin-Boltzmann (KB) model

[23]. To identify the models offline, researchers typically employ static signals such as the stress relaxation response of the tissue. Since the models are inherently dynamic, the static signals previously used to identify the system may not have reflected the tissue’s actual behaviour. However, in general, surgical robotic systems are teleoperated, so the haptic feedback is generated using online measurements. Previous models have been parameterized using online recursive algorithms, or modern observer-based control policies have been used to provide robustness to model uncertainty [19–22, 24]. In surgical simulation, the real environment is abstracted to a virtual simulation. Without sensor measurements, the models used in simulation may require more accuracy than the ones implemented in surgical robotics. Higher accuracy would necessitate that the signals generated to identify these models would be dynamic to reflect the true nature of the tissue system.

Previous studies on modelling tissue force feedback for surgical simulation of the access-gaining step of an MI surgery have focused on measuring the force response from cadavers [25, 26]. In a study by El-Monajjed *et al.*, the force required to gain access with a probe for a MI spine surgery was measured [25, 27]. This study provided insight into the force response of the tissue layers and provided a comprehensive dictionary of forces during tool-tissue interaction. While using cadaveric measurements provides a realistic ground truth, the signals used to determine the tissue force feedback in this study were largely static, with the dynamic behaviour of the tissue being inferred from stress relaxation response curves [25, 27]. This study used a physics based approach in that it directly measured forces from a realistic ground truth, however considering dynamic signals to realize a system model may provide more insight into the tissue force feedback behaviour. The measurements were then implemented into a surgical simulator as a force feedback algorithm [28, 29]. This was done considering multiple different force feedback scenarios that were fit with a second order polynomial and integrated into the surgical simulation platform [28, 29]. While this algorithm considers multiple different types of forces, it provides fits to the cadaveric curves, whereas modelling the system instead as a dynamical equation could fit to the tissue behaviour while

also potentially simplifying the force feedback algorithm.

An additional concern is how closely the behaviour of the force feedback model must match the system to ensure the realism perceived by the operator. Previous studies have examined the tradeoff between computational complexity and graphics within surgical simulation [30]. However limited comparable studies currently exist for the tradeoff between tissue model accuracy and the realism in the force feedback provided to the operator. Kim *et al.* examined force feedback model fidelity when there is no force feedback and with force feedback modelled as linear and non-linear functions [31]. They found by assessing the learning curve of the operators of a laparoscopic surgical simulator that the highest fidelity was observed in the nonlinear function [31]. However, the functions they used had no terms that evolve with time. The performance of such dynamic changes in the system within the context of surgical simulation is yet to be assessed. Lastly, the boundaries of human perception have been quantified for just noticeable differences between two tactile stimuli at the fingertips as a change of 7% for forces between 2 N and 10 N [32]. Transiently, the differences experienced with respect to the MI spine surgical simulation remain undefined.

The purpose of the present study is to identify and assess force feedback models of soft tissue during the access-gaining step of an MI spine interbody-fusion surgery. The objectives of this study are:

- to identify the tissue force feedback response as the dynamic systems outlined in Figure 3.2 and,
- to examine the tradeoff between the accuracy of the force feedback models with respect to the tissue dynamic behaviour, and how the models are rated by the operator when programmed into a surgical simulator.

The objectives were addressed by first conducting system identification on a tissue analogue. Then by programming the identified models into a surgical simulator and having participants rank how well the models mimicked the behaviour of the tissue analogue.

3.2.3 Methods

System identification experiments were performed on a rubber tissue analogue (Lumbar Spine Demonstrator, The Chamberlain Group). The tissue analogue was previously found to be suitable for capturing the surgical forces during the MI spine surgery for the incision size used in this work [33]. Three models were fit to the system using system identification methods. First, two models were grey-box models that were selected based on the viscoelastic properties of the tissue. The grey-box model components are arranged in the different arrays seen in Figure 3.2. The array configurations dictate the ordinary differential equations that describe the inherent tissue force feedback dynamics used to formulate the system identification problem. The third model was a black-box higher-order model that was selected based on the dynamic equation with the best error metrics. The system identification procedure and statistical analysis was done using Python (3.10) and the procedure can be completed using established libraries and the equations outlined in this study. The IL model was also built to be less reflective of tissue properties with an inverted force vector and no dynamic component. The models were programmed into an Entact W3D haptic device (Guelph, Canada) to test how they performed in simulation. The Entact W3D is a three degree-of-freedom impedance controlled manipulator robot with three DC motors (maximum transient force of 15 N), and a surgical tool mounted at roughly the center of mass of the end-effector. The haptic device uses an Ethernet communication protocol with a game engine hosted on an MSI GT73VR 7RF (MSI) Core i7 3.5 GHz 64 GB RAM laptop and a NVIDIA GTX 1080 GPU to support the simulation environment. Participants were recruited to test the different models on the haptic device and determine which ones best replicated the identified system. Ethical approval for experiments with human participants was obtained through the appropriate local ethical bodies (McGill University IRB A03-M15-20A/ eRAP 20-03-019, Amendment approved on 22 August 2022).

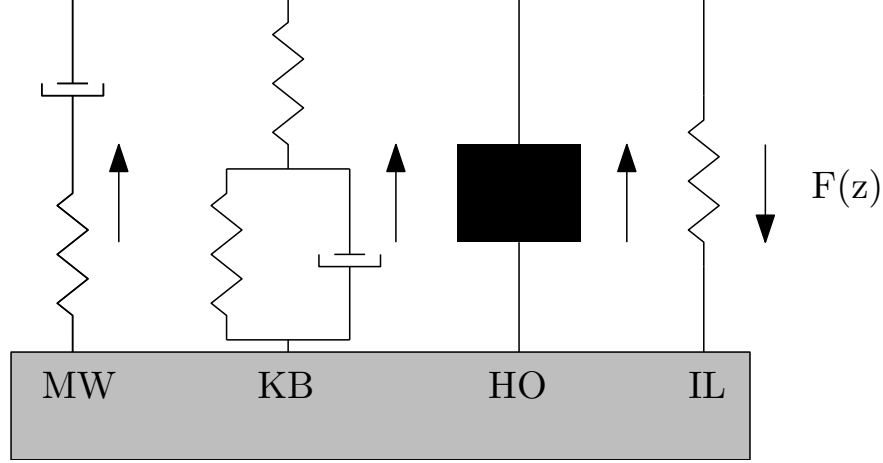


Figure 3.2: Schematics of tissue force feedback models under consideration from left to right: the Maxwell (MW), the Kelvin Boltzmann (KB), the blackbox higher-order (HO), and the inverted linear (IL) model.

3.2.3.1 System Identification

In previous studies, the haptic device used in this work was employed for simulation of the access-gaining step of an MI spine surgery [5, 29]. In this work the position of the tool tip in the z -direction with respect to time was obtained from those previous trials conducted with surgeons. The power spectral density of these curves is assessed using Welch's method to determine an approximate signal bandwidth for the system identification experiments.

Three broadband excitation signals were then generated to excite the tissue across the bandwidth of interest. First is a Schroeder multisine signal

$$u(t) = \sum_{k=1}^F A \cos(2\pi f_k t + \phi_k), \quad (3.1)$$

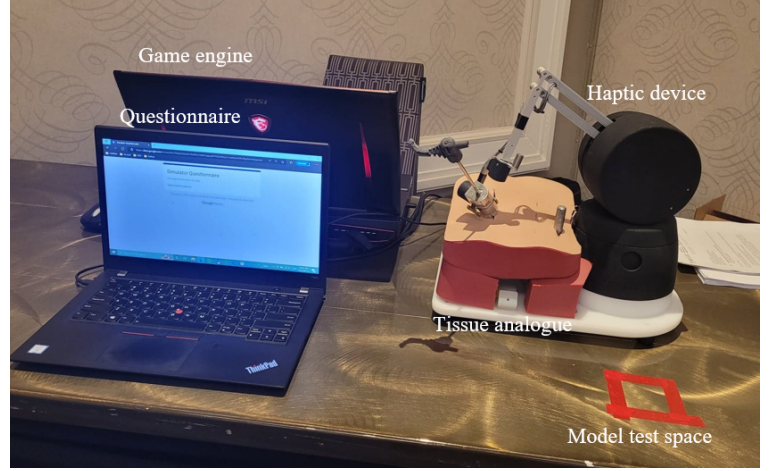
with the Schroeder phases ϕ_k and the increments of the frequency f_k [34]. Second is a chirp signal

$$u(t) = A \sin((at + b)t), \quad (3.2)$$

where A is the amplitude, and a and b are functions of the highest and lowest frequencies of the signal [34]. Lastly, a band-limited Gaussian noise signal was generated in Python using a Gaussian noise function and applying a low-pass filter [34]. These signals were used



(a)



(b)

Figure 3.3: (a) Setup for the system identification experiments with the tool tip for the surgery fixed to the top and the tissue analogue fixed to the bottom and tool tip direction indicated. (b) Experimental setup used by study participants in the simulation that consisted of the game engine, questionnaire, haptic device, tissue analogue, and model test space.

because they can be designed to excite across the entire bandwidth of frequencies that were determined from the power spectral density of the surgeon data.

The rubber tissue analogue with a small incision was mounted on an Instron for unilateral material testing (ElectroPuls® E10000 Linear-Torsion, 95 Instron, MA, USA). The surgical tool tip was fixed to the top of the MTS and the analogue was fixed to the bottom as in Figure 3.3a. The input signal was the tool tip position in the z -direction moving throughout the tissue as indicated by the broadband excitation signal, and the output signal was the corresponding force response from the tissue analogue.

The two grey-box models were fit to the system as discrete-time transfer functions, where a_k and b_k represent nominal parameter values, and z is associated with the z -transform. The Maxwell (MW) model

$$H(z) = \frac{b_0}{z - a_0}, \quad (3.3)$$

and the Kelvin Boltzmann (KB) model is

$$H(z) = \frac{b_1 z - b_0}{z - a_0}. \quad (3.4)$$

The Kelvin-Voigt model, which consists of a spring and dashpot in parallel, is not considered in this study as it forms an improper transfer function

$$H(z) = b_1 z - b_0. \quad (3.5)$$

An inverted linear (IL) model was also included to provide a less realistic model for the soft tissue system. This model was selected as it contained only a static spring and the force was in the opposite direction from the other models. This model is built as a linear increase in force going from 0 N to 5 N, which is the maximum static capabilities of the haptic device motors.

The models are fit to the system using the autoregressive with exogenous variables (ARX) model [35]. Where the output is represented as the linear transformation of a time window of input (u_k) and output (y_k) points applied to a vector of time-invariant parameters

$$\underbrace{\begin{bmatrix} y_N \\ y_{N-1} \\ \vdots \\ y_{n+1} \\ y_n \end{bmatrix}}_{\mathbf{b}} = \underbrace{\begin{bmatrix} -y_{N-1} \dots -y_{N-n} & u_{N-n+m} \dots u_{N-n} \\ -y_{N-2} \dots -y_{N-n-1} & u_{N-n-1+m} \dots u_{N-n-1} \\ \vdots & \ddots & \vdots & \vdots & \ddots & \vdots \\ -y_n & \dots & -y_1 & u_{1+m} & \dots & u_1 \\ -y_{n-1} \dots & -y_0 & u_m & \dots & u_0 \end{bmatrix}}_{\mathbf{A}} \underbrace{\begin{bmatrix} b_{n-1} \\ \vdots \\ b_0 \\ a_m \\ \vdots \\ a_0 \end{bmatrix}}_{\mathbf{x}}. \quad (3.6)$$

The original formulation for the ARX system identification problem uses a linear least squares cost function [35]. However, a regularization term is added to the cost function as it improves the numerical conditioning and may also encourage system stability by favouring smaller norms of the solution. Additionally, the regularization term can improve the bias-variance problem observed in classical system identification using the ARX model,

$$\min_{\mathbf{x}} \left(\|\mathbf{Ax} - \mathbf{b}\|_2^2 + \|\mathbf{\Gamma x}\|_2^2 \right), \quad (3.7)$$

where $\mathbf{\Gamma} = \alpha \mathbf{1}$ is the Tikhonov matrix and α is the ridge regression coefficient that dictates

to what extent a small solution norm is favoured [36]. The solution to equation 3.7 is

$$\mathbf{x} = (\mathbf{A}^\top \mathbf{A} + \mathbf{\Gamma}^\top \mathbf{\Gamma})^{-1} \mathbf{A}^\top \mathbf{b}. \quad (3.8)$$

The Tikhonov matrix is created using a grid search. The grid is designed to be an evenly spaced geometric progression along a logarithmic scale to give preference to smaller values of α , where values of up to 100 were searched through. This design choice is made because at high values of α the solution becomes essentially compressed to zero, due to the cost function overvaluing a small solution norm.

To build the higher-order (HO) model the grid search is extended to three dimensions to optimize the model hyperparameters. The other two dimensions represent the number of terms in the numerator and the number of terms in the denominator of the discrete-time transfer function of the form

$$H(z) = \frac{b_m + \dots + b_1 z^{-m+1} + b_0 z^{-m}}{1 + a_{n-1} z^{-1} + \dots + a_0 z^{-n}}. \quad (3.9)$$

The search space is confined to only consider biproper and proper transfer functions. For each model several error metrics are evaluated as well as the conditioning and stability of the resulting transfer function. The search is performed for each excitation signal for model training with the remaining excitation signals used as testing datasets. The error metrics that are evaluated for each model are the mean of the residuals

$$\bar{y} = \frac{1}{N} \sum_{k=1}^N |y_k - \hat{y}_k|, \quad (3.10)$$

where N represents the number of measurements in \mathbf{y} , fit ratio (FIT)

$$\text{FIT} = \left(1 - \frac{\sqrt{\frac{1}{N} \sum_{k=1}^N (\hat{y}_k - y_k)^2}}{\sigma_y} \right) \times 100, \quad (3.11)$$

$$\sigma_y = \sqrt{\frac{1}{N} \sum_{k=1}^N (y_k - \bar{y})^2},$$

and the percent variance accounted for (%VAF) [18, 37, 38]

$$\%VAF = \left(1 - \frac{\text{var}(\hat{y}_k - y_k)}{\text{var}(y_k)}\right) \times 100. \quad (3.12)$$

The normalized mean squared error (NMSE) for both the testing and training datasets is also assessed [37, 38]

$$\text{NMSE} = \frac{\frac{1}{N} \|\mathbf{b} - \mathbf{A}\mathbf{x}\|_2^2}{\frac{1}{N} \|\mathbf{b}\|_2^2}. \quad (3.13)$$

In addition to the error metrics, uncertainty in the system and the solution are also evaluated. The numerical conditioning is used because a small condition number represents when the system is given a small relative input error it will result in a small relative output error. Whereas a poorly-conditioned solution will amplify small relative input errors

$$\text{cond}(\mathbf{A}) = \frac{\sigma_{\max}(\mathbf{A})}{\sigma_{\min}(\mathbf{A})}, \quad (3.14)$$

where $\sigma_{\min}(\mathbf{A})$, and $\sigma_{\max}(\mathbf{A})$ represent the minimum and maximum singular values of the \mathbf{A} -matrix respectively [18]. The relative uncertainty (RU) of the parameters was evaluated as well by using

$$\mathbf{\Sigma} \approx \frac{1}{N - (n + m + 1)} \|\mathbf{b} - \mathbf{A}\mathbf{x}\|_2^2 (\mathbf{A}^\top \mathbf{A})^{-1}, \quad (3.15)$$

where $\mathbf{\Sigma}$ has the diagonal elements σ_i^2 representing the uncertainty for each parameter [38]. The variables n , and $m + 1$ represent the number of terms in the discrete-time transfer function numerator and denominator respectively. The maximum relative uncertainty (MRU) is then the maximum of

$$\text{RU} = \frac{\sigma_i}{|x_i|} \times 100 \quad (3.16)$$

associated with the solution parameters [39].

The best performing model is picked according to the %VAF since sorting according to that metric yielded the best results from the other metrics as well. The best performing blackbox model with reasonable numerical conditioning was then selected.

3.2.3.2 Simulator Trials

The identified models were integrated into the haptic manipulator platform using the discrete-time state-space representation as

$$\mathbf{x}_k = \mathbf{A}\mathbf{x}_{k-1} + \mathbf{B}u_{k-1}, \quad (3.17)$$

$$y_k = \mathbf{C}\mathbf{x}_k + \mathbf{D}u_k. \quad (3.18)$$

Since higher-order models required more steps back in time, the higher-order the model, the more sensitive it was to noise and uncertainty in measurement such as errors in encoder measurements and small perturbations in end-effector movement. Therefore, a moving average about the three previous points on the position measurements was implemented to prevent chattering from the haptic device.

The integrated models were then tested with participants. The participants were recruited from attendees of an international conference held by the Fascia Research Congress, as such they were a selection of research scientists, practicing healthcare professionals, and individuals with an interest in soft tissue composition and dynamics.

The experimental setup in Figure 3.3b consisted of a haptic device, the game engine, the questionnaire, and the model test space. Participants were given up to 45s to puncture the tissue analogue without any force feedback provided from the haptic device, then they were told to puncture the model test space in the same way. The force feedback in the test space began approximately 40 mm above the table to reflect the distance they would puncture in the analogue. For each force feedback model the participants were given up to 30 seconds to try the model then they filled out the corresponding question in the questionnaire.

The two questions in the survey that addressed the objectives of this study were as follows:

1. "The forces experienced during the simulation were similar to those of what I felt on the rubber analogue";
2. "The model that most closely matched the rubber tissue analogue was:".

The first question was given for each model with a 5-point Likert scale ranging from strongly

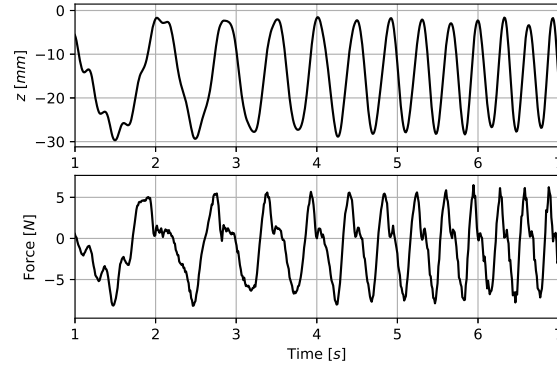
disagree-1 to strongly agree-5 [40, 41]. The second question was asked at the end of the experiment so participants could select which model they thought performed the best. The results from the questionnaire were evaluated using descriptive statics of mode and median as well as non-parametric inferential statistical tests namely the Kruskal-Wallis H-test and Mann-Whitney U-Test [42–44]. The results were considered to have statistical significance at a p-value of < 0.05 and strong statistical significance at a p-value of < 0.001 . A Bonferroni-Holm correction was also applied for $\alpha < 0.05$ to ensure statistical significance for multi-group comparisons.

3.2.4 Results

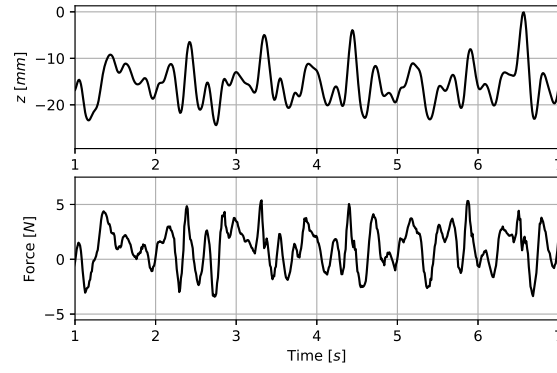
3.2.4.1 System Identification

The frequency bandwidth from trials conducted with the surgical simulator was found to be up to approximately 2.5 Hz. The chirp and Schroeder multisine were then generated up to the Nyquist rate of 5 Hz and the Gaussian noise was filtered to obtain only noise up to the Nyquist rate as well. Therefore the signals were designed to excite the system across a bandwidth of $[0, 5]$ Hz. The signals were then programmed into the MTS at 100 Hz, which was the approximate sampling frequency of the simulation environment of the surgical simulator. The chirp and Gaussian noise signals were sampled up to 10s, but the Schroeder multisine was sampled up to 100s to capture the periodic nature of the signal. A segment of each broadband excitation input signal and the corresponding output were presented in Figure 3.4. Due to the length of the Schroeder multisine only a segment of the data was plotted in Figure 3.4 for clarity.

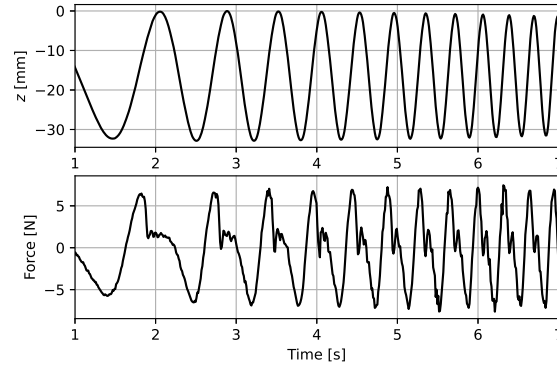
After performing the optimization procedure defined in equation (3.7), the resulting error metrics and optimized ridge regression coefficients were obtained. The results are presented in Table 3.1. The models with the best FIT and %VAF were selected to program into the haptic device, which were obtained from the models trained with the multisine data. The resulting model outputs were then plotted in Figure 3.5.



(a)



(b)



(c)

Figure 3.4: A segment $[1, 7]$ s of the dynamic input (z) and output ($Force$) signals obtained from the system identification experiments. (a) Chirp, (b) Gaussian noise, (c) Shroeder multisine.

Table 3.1: Error metrics obtained during the exhaustive search for the MW, KB and HO models. The metrics obtained were: the condition number the percent variance accounted for (%VAF), the maximum relative uncertainty of the parameters (MRU), the FIT ratio, the mean residuals, the normalized mean squared error for the testing and training data and the ridge regression coefficient (alpha).

	Model	Condition Number	%VAF	MRU (%)	FIT	Mean Residuals	NMSE train	NMSE test 1	NMSE test 2	Alpha
Multisine	MW	1.95	12.24	0.02	6.32	2.77	0.29	0.44	0.32	39.44
	KB	29.38	81.16	0.03	56.59	1.25	0.04	0.05	0.06	0.27
	4th order	2086.15	82.64	4.99	58.33	1.24	0.03	0.03	0.05	0.02
Gaussian Noise	MW	1.92	2.09	0.11	1.05	1.65	0.05	0.07	0.09	0.48
	KB	44.46	66.16	0.24	41.83	0.83	0.02	0.05	0.06	0.19
	4th order	2734.23	67.44	613.42	42.94	0.78	0.02	0.03	0.05	0.05
Chirp	MW	1.56	6.92	0.43	3.52	3.13	0.35	0.43	0.33	17.48
	KB	27.68	70.21	0.44	45.42	1.74	0.06	0.03	0.04	0.00
	5th order	3481.04	72.55	2428.57	47.61	1.72	0.04	0.03	0.03	0.03

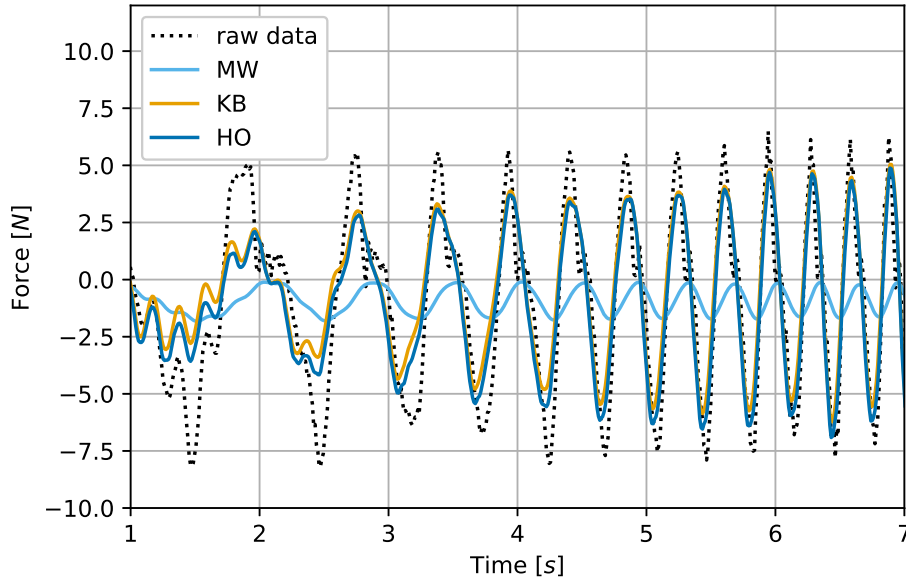


Figure 3.5: A segment of multisine data from the tissue force response between $[1, 7]$ s compared to the corresponding output from the Maxwell (MW), Kelvin Boltzmann (KB), and higher-order (HO) models.

Table 3.2: On the left side are the descriptive statistics of the Likert scale data as well as the percentage of participants ($N = 45$) who selected that model as the best performing once completing the experiment. On the right are the p-values from the Mann-Whitney U-test between the model ratings from study participants.

	Median	Mode	Mode Count	% Best	MW Model	KB Model	HO Model
IL model	2	2	16	4.40%	p <0.05	p <0.001	p <0.001
MW model	3	3	15	31.10%	-	p <0.05	p <0.05
KB model	4	4	14	26.70%	-	-	0.8
HO model	4	4	16	37.80%	-	-	-

3.2.4.2 Simulator Trials

There were a total of 45 participants in the study. Of the study participants 75.6% self-classified as clinicians, 15.6% had practiced dry needling, 13.3% had practiced acupuncture, and 93.3% had practiced palpation. Additionally, 11.1% of participants reported having less than 5 years experience in their field, and 35.6% reported having over 20 years experience in their field.

The Likert scale was treated as ordinal data, as such the descriptive statistics were the median and mode [42, 43]. Table 3.2 summarized the results from the descriptive statistics obtained from the study population ($N = 45$) and the percentage of participants who rated that model as the best performing. The highest percentage of individuals rated the HO model as the best. The median and mode for the KB and HO models were the highest as well, with the mode count being higher for the HO model than the KB model.

The Kruskal-Wallis H-test yielded a p-value < 0.05, allowing the null hypothesis to be rejected indicating that the population medians between all groups were not equal. Testing between groups using the Mann-Whitney U-test yielded the p-values in Table 3.2.

The results indicated significant differences in the ratings between the linear model to the MW model, and the KB model. The KB model and HO model did not show statistically significant differences in their population medians. After the Bonferroni-Holm correction was applied results remained statistically significant for $\alpha < 0.05$.

3.2.5 Discussion

The purpose of the study was to simulate force feedback of soft tissues in the access gaining step of an MI spine surgery. This was accomplished by first identifying the force feedback from a tissue analogue using the dynamic input and output signals seen in Figure 3.4. These signals were designed to excite the tissue system across a bandwidth of up to 2.5 Hz. This bandwidth was determined from the power spectral density of the position data obtained from the haptic device from simulations conducted with surgeons during the access gaining step of the MI spine surgery. The limit represents the maximum frequency at which the surgeons would excite the tissue resulting in a force response. The excitation signal that produced the best error metrics in the system identification process was the Schroeder multisine. This signal was longer than the others to capture its periodic nature. The longer length of the signal may have contributed to the better error metrics that were observed.

From the input and output data organized into equation (3.6) the MW, KB, and HO models were identified using equation (3.8). The final models compared to the original data produced the best error metrics from the HO black box model. This was expected since the HO blackbox model had the highest number of elements that allows for the most tuning in the parameters to achieve the closest fit to the original data. Additionally, since the behaviour being modelled is not simply the viscoelasticity of the tissue but also the force feedback dynamics of the access-gaining step of the MI spine surgery, the added terms in the HO model may allow for additional tool-tissue interaction dynamics to be modelled in addition to the viscoelastic tissue behaviour. However, the HO model increased the accuracy of the overall results only slightly compared to the KB model. When referencing Table 3.1 the HO model performed the best when considering NMSE (both testing and training), %VAF, FIT, and the mean residuals compared to the MW and KB models. However, the HO model had the poorest conditioning and relative uncertainty. This means that while the HO model may have provided a better fit to the dynamic behaviour, the parameter values may be more uncertain and be easily influenced by errors in the system identification experiments. The

HO model better satisfied the objectives of the experiment, however, with minimal tradeoff in accuracy, the KB model provided a less uncertain estimation of the system's dynamic behaviour. Overall, the quantitative metrics from the system identification experiments demonstrate that the linear dynamic models can be fit to the input and output data with a reasonable amount of accuracy and uncertainty.

The final objective was to determine if the models needed to accurately replicate the dynamic behaviour of the tissue when used in a surgical simulator. The results in Table 3.2 indicated significant improvement in the ratings going from the IL model to the MW model, and the KB model. The KB model and HO model did not show statistically significant differences in their population medians. However, it can be noted that in Table 3.2 the mode count was higher for the HO model and the percentage of people who rated it the best was the highest. This may indicate that the HO model could have been preferred over the others. Additionally, there may be other factors that influenced the selection of one model over another. For example, some participants noted that higher forces in the haptic device felt mechanical, despite those forces being closer in magnitude to those experienced in the tissue analogue. This could explain why some selected the MW model as their preferred choice, as it demonstrated the dynamic behaviour of the tissue but at lower magnitudes than the KB or HO models. It should also be noted that the IL model had the lowest percentage of people who rated it as the best, indicating that the implemented/selected haptic feedback model should mimic the behaviour of the tissues in order to provide realistic tactile and force feedback during surgical simulator training. The qualitative results validate the system identification approach using dynamic signals and models when implemented into a spine surgical simulator.

There were some limitations to the study. Firstly, the focus of this study was to evaluate dynamic models of the tissue system in a spine surgical simulator, however this work also utilized a static IL model, in addition to the dynamic MW, KB, and HO models. The IL model was used to compare the responses from participants for a less representative

tissue model to the ones built to be representative of the tissue using system identification. Extending beyond the contributions of this work, future studies should examine additional models that do not include components that evolve with time, but that are more representative of the tissue behaviour than the IL model, to evaluate how the performance compares between static models and dynamic ones. Secondly, the models used for grey-box and black-box identification were assumed to be linear dynamic equations, however, previous studies have found that real soft tissue behaviour may be modelled as nonlinear [19, 45]. Additionally, the soft tissue was modelled as uniform, however, multiple different soft tissues are penetrated during spine surgeries which may have varying material properties [46]. Using a tissue analogue for the experiments allowed both objectives of the study to be addressed. However, using system identification methods with animal or cadaveric models in future studies may provide more insight into the non-linear behaviour and may indicate any changing properties of the tissue throughout the access-gaining step. Additionally, models identified from animal or cadaveric tissues could also be compared to the ones developed from rubber analogues to see how the force feedback dynamics compare between different materials used in surgical training. Lastly, the force feedback in the study was restricted to a single degree of freedom to ensure consistency in the motion of the participants when using the haptic device to evaluate the models. However, extending the models to multiple degrees of freedom could provide additional insight on the overall behaviour of the tissue and could allow for the opportunity to model its anisotropic properties [47].

Overall, the contributions of this work demonstrated that the better the model captured the dynamic behaviour of the signals in Figure 3.4 dictated by the error metrics in Table 3.1, the more realistically it was perceived by the operator within the limitations of the results presented in Table 3.2. The objectives were validated both quantitatively from the numerical results in the system identification experiments, and qualitatively using the results from the surveyed study participants. In a broader context this study demonstrates that to adequately model the force feedback of soft tissues for surgical simulation it may be necessary to consider

the dynamics. Additionally, by modelling a dynamical equation, the results have real physical interpretations that may make the implementation of the models tractable in other related systems. With further work on understanding the physical interpretation of the model parameters the models could potentially be tuned to the force feedback dynamics of soft tissues for other surgical simulators as well. In order to create such scalable systems they may need to first be accurate to the real force feedback dynamics as outlined in this study. Modelling the force feedback dynamics involves both generating signals along a bandwidth of frequencies to realize the system model, and also ensuring the system models themselves contain components that evolve with time.

3.2.6 Conclusion

This study modelled tissue force response during the access-gaining step of an MI spine surgery using classical system identification techniques. The models were programmed into a simulation and rated by participants. The results demonstrated that the tissue force response may need to be modelled using dynamic input and output signals. The results from the experiments that were conducted with participants demonstrate that the models may also need to accurately replicate the dynamic behaviour of tissue to provide realistic tactile feedback when programmed into a haptic device for surgical simulation. Overall, the study demonstrated the benefits of both accurate and dynamic models to be used in the simulation of the access-gaining step of an MI spine surgery.

3.2.7 Acknowledgments

The authors acknowledge the support obtained from Natural Science and Engineering Research Council of Canada (funding number: 258507). There are no conflicts of interest to declare.

3.2.8 References

- [1] H. V. Chorney, J. R. Forbes, and M. Driscoll, “System identification and simulation of soft tissue force feedback in a spine surgical simulator”, *Computers in Biology and Medicine*, p. 107 267, 2023.
- [2] S. V. Kotsis and K. C. Chung, “Application of see one, do one, teach one concept in surgical training”, *Plastic and Reconstructive Surgery*, vol. 131, no. 5, p. 1194, 2013.
- [3] A. G. Gallagher *et al.*, “Virtual reality simulation for the operating room: Proficiency-based training as a paradigm shift in surgical skills training”, *Ann. of Surgery*, vol. 241, no. 2, p. 364, 2005.
- [4] C. E. Buckley, D. O. Kavanagh, O. Traynor, and P. C. Neary, “Is the skillset obtained in surgical simulation transferable to the operating theatre?”, *The Amer. J. of Surgery*, vol. 207, no. 1, pp. 146–157, 2014.
- [5] S. Alkadri *et al.*, “Utilizing a multilayer perceptron artificial neural network to assess a virtual reality surgical procedure”, *Comput. in Biol. and Med.*, vol. 136, p. 104 770, 2021.
- [6] S. M. Werz, S. Zeichner, B.-I. Berg, H.-F. Zeilhofer, and F Thieringer, “3d printed surgical simulation models as educational tool by maxillofacial surgeons”, *Eur J Dent Educ.*, vol. 22, no. 3, e500–e505, 2018.
- [7] C. L. Cheung, T. Looi, T. S. Lendvay, J. M. Drake, and W. A. Farhat, “Use of 3-dimensional printing technology and silicone modeling in surgical simulation: Development and face validation in pediatric laparoscopic pyeloplasty”, *J. Surg. Educ.*, vol. 71, no. 5, pp. 762–767, 2014.
- [8] P. Li, Z. Yang, and S. Jiang, “Tissue mimicking materials in image-guided needle-based interventions: A review”, *Mater. Sci. Eng. C*, vol. 93, pp. 1116–1131, 2018.

- [9] B. Stott and M. Driscoll, “Face and content validity of analog surgical instruments on a novel physics-driven minimally invasive spinal fusion surgical simulator”, *Med. & Bio. Eng. & Comput.*, vol. 60, no. 10, pp. 2771–2778, 2022.
- [10] K. Rangarajan, H. Davis, and P. H. Pucher, “Systematic review of virtual haptics in surgical simulation: A valid educational tool?”, *J. of Surgical Educ.*, vol. 77, no. 2, pp. 337–347, 2020.
- [11] K. R. Woods, J. B. Billys, and R. A. Hynes, “Technical description of oblique lateral interbody fusion at l1–l5 (olif25) and at l5–s1 (olif51) and evaluation of complication and fusion rates”, *The Spine J.*, vol. 17, no. 4, pp. 545–553, 2017.
- [12] H. Abbasi and A. Abbasi, “Oblique lateral lumbar interbody fusion (ollif): Technical notes and early results of a single surgeon comparative study”, *Cureus*, vol. 7, no. 10, 2015.
- [13] M. Griffin, Y. Premakumar, A. Seifalian, P. E. Butler, and M. Szarko, “Biomechanical characterization of human soft tissues using indentation and tensile testing”, *JoVE (J. of Visualized Experiments)*, no. 118, e54872, 2016.
- [14] M. Khadem, B. Fallahi, C. Rossa, R. S. Sloboda, N. Usmani, and M. Tavakoli, “A mechanics-based model for simulation and control of flexible needle insertion in soft tissue”, in *2015 IEEE Int. Conf. Robot. Automat. (ICRA)*, IEEE, 2015, pp. 2264–2269.
- [15] M. Alber *et al.*, “Integrating machine learning and multiscale modeling—perspectives, challenges, and opportunities in the biological, biomedical, and behavioral sciences”, *NPJ Digit. Medicine*, vol. 2, no. 1, pp. 1–11, 2019.
- [16] L. Ljung *et al.*, “Theory for the user”, *System Identification*, 1987.
- [17] M. B. Tischler, *System identification methods for aircraft flight control development and validation*. Routledge, 2018.
- [18] D. T. Westwick and R. E. Kearney, *Identification of nonlinear physiological systems*. John Wiley & Sons, 2003, vol. 7.

- [19] A. Pappalardo, A. Albakri, C. Liu, L. Bascetta, E. D. Momi, and P. Poignet, “Hunt–crossley model based force control for minimally invasive robotic surgery”, *Biomed. Signal Process. and Control*, vol. 29, pp. 31–43, Aug. 2016.
- [20] P. Moreira, N. Zemiti, C. Liu, and P. Poignet, “Viscoelastic model based force control for soft tissue interaction and its application in physiological motion compensation”, *Comput. Methods and Programs in Biomedicine*, vol. 116, no. 2, pp. 52–67, 2014.
- [21] M. Ferro, C. Gaz, M. Anzidei, and M. Vendittelli, “Online needle-tissue interaction model identification for force feedback enhancement in robot-assisted interventional procedures”, *IEEE Trans. on Med. Robot. and Bionics*, vol. 3, no. 4, pp. 936–947, 2021.
- [22] L. Barbé, B. Bayle, M. de Mathelin, and A. Gangi, “In vivo model estimation and haptic characterization of needle insertions”, *The Int. J. of Robot. Res.*, vol. 26, no. 11-12, pp. 1283–1301, 2007.
- [23] T. H. Lee, W. Liang, C. W. de Silva, and K. K. Tan, *Force and Position Control of Mechatronic Systems*. Springer International Publishing, 2021. [Online]. Available: <https://doi.org/10.1007/978-3-030-52693-1>.
- [24] A. Haddadi and K. Hashtrudi-Zaad, “Real-time identification of hunt-crossley dynamic models of contact environments”, *IEEE Trans. on Robot.*, vol. 28, no. 3, pp. 555–566, 2012.
- [25] K. El-Monajjed and M. Driscoll, “Analysis of surgical forces required to gain access using a probe for minimally invasive spine surgery via cadaveric-based experiments towards use in training simulators”, *IEEE Trans. on Biomed. Eng.*, vol. 68, no. 1, pp. 330–339, 2020.
- [26] D. Yua, X. Zhengb, M. Chenc, and S. G. Shend, “Preliminarily measurement and analysis of sawing forces in fresh cadaver mandible using reciprocating saw for reality-based haptic feedback”, *J. of Craniofacial Surgery*, vol. 23, no. 3, pp. 925–929, 2012.

- [27] B. Brahmi, I. E. Bojairami, J. Ghomam, M. Habibur Rahman, J. Kovecses, and M. Driscoll, “Skill learning approach based on impedance control for spine surgical training simulators with haptic playback”, *Proc. Inst. Mech. Eng., I: J. Syst. Control Eng.*, p. 09 596 518 221 133 425, 2022.
- [28] K. El-Monajjed and M. Driscoll, “Haptic integration of data-driven forces required to gain access using a probe for minimally invasive spine surgery via cadaveric-based experiments towards use in surgical simulators”, *J. of Comput. Sci.*, vol. 60, p. 101 569, 2022.
- [29] S. Patel, S. Alkadri, and M. Driscoll, “Development and validation of a mixed reality configuration of a simulator for a minimally invasive spine surgery using the workspace of a haptic device and simulator users”, *Biomed. Res. Int.*, vol. 2021, 2021.
- [30] T. Wang, *A comparative study to balance the computational complexity and virtual graphics in a novel surgical simulator*. McGill University (Canada), 2020.
- [31] H. K. Kim, D. W. Rattner, and M. A. Srinivasan, “Virtual-reality-based laparoscopic surgical training: The role of simulation fidelity in haptic feedback”, *Comput. Aided Surgery*, vol. 9, no. 5, pp. 227–234, 2004.
- [32] X.-D. Pang, H. Z. Tan, and N. I. Durlach, “Manual discrimination of force using active finger motion”, *Perception & Psychophysics*, vol. 49, no. 6, pp. 531–540, 1991.
- [33] K. El-Monajjed, “Implementation of a virtual reality module for gaining surgical access via planned oblique lateral lumbar interbody fusion”, 2021.
- [34] R. Pintelon and J. Schoukens, “System identification a frequency domain approach”, in Hoboken, NJ, USA: John Wiley & Sons, Inc., 2001, pp. 1–737.
- [35] T. Hsia, *System Identification: Least-squares Method*. Lexington, MA: Lexington Books, 1978.
- [36] L. Ljung, T. Chen, and B. Mu, “A shift in paradigm for system identification”, *Int. J. of Control*, vol. 93, no. 2, pp. 173–180, 2020.

- [37] H. Muroi and S. Adachi, “Model validation criteria for system identification in time domain”, *IFAC-PapersOnLine*, vol. 48, no. 28, pp. 86–91, 2015.
- [38] J. P. Hespanha, *Advanced undergraduate topics in control systems design*, 2019.
- [39] J. Norton, *An introduction to identification*. Academic Press, 1986.
- [40] J. LeBlanc, C. Hutchison, Y. Hu, and T. Donnon, “Feasibility and fidelity of practising surgical fixation on a virtual ulna bone”, *Can. J. of Surgery*, vol. 56, no. 4, E91, 2013.
- [41] E. M. McDougall, “Validation of surgical simulators”, *J. of Endourology*, vol. 21, no. 3, pp. 244–247, 2007.
- [42] D. Bertram, “Likert scales”, *CPSC 681 – Topic Report*, vol. 2, no. 10, pp. 1–10, 2007.
- [43] I. E. Allen and C. A. Seaman, “Likert scales and data analyses”, *Qual.Prog.*, vol. 40, no. 7, pp. 64–65, 2007.
- [44] H. N. Boone and D. A. Boone, “Analyzing likert data”, *J. of Extension*, vol. 50, no. 2, pp. 1–5, 2012.
- [45] A. Bianco, R. Zonis, A.-M. Lauzon, J. R. Forbes, and G. Ijpma, “System identification and two-degree-of-freedom control of nonlinear, viscoelastic tissues”, *IEEE Trans. on Biomed. Eng.*, 2022.
- [46] I. E. Bojairami, A. Hamedzadeh, and M. Driscoll, “Feasibility of extracting tissue material properties via cohesive elements: A finite element approach to probe insertion procedures in non-invasive spine surgeries”, *Med. & Biol. Eng. & Comput.*, vol. 59, no. 10, pp. 2051–2061, 2021.
- [47] G. Picinbono, H. Delingette, and N. Ayache, “Nonlinear and anisotropic elastic soft tissue models for medical simulation”, in *Proc. 2001 ICRA IEEE Int. Conf. on Robot. and Automat. (Cat. No. 01CH37164)*, IEEE, vol. 2, 2001, pp. 1370–1375.

3.2.9 Summary

Surgical simulators offer a means to train surgical skills at a low cost. This study focuses on developing and evaluating force feedback models for soft tissue during the access-gaining step of a minimally invasive spine interbody fusion surgery. During the access-gaining step the surgeon relies almost entirely on somatosensory feedback, so the force feedback models are important in a simulation setting. Previous studies have focused largely on static methods and this study examines force feedback tissue dynamics using system identification.

The models were built using data collected from tests with a tissue analogue. From the input and output signals, three models were fit to the system. Two models were grey-box models, the Kelvin Boltzmann (KB) and Maxwell (MW) models, which were selected based on the viscoelastic properties of the tissue. The third model was a black-box higher-order (HO) model that was selected based on the dynamic equation with the best error metrics. The systems were identified using classical system identification and Tikhonov regularization. The identified models were integrated into a haptic device and tested with study participants who rated them based on how they matched the behaviour of the rubber tissue analogue. The study participants were a selection of research scientists, practicing healthcare professionals, and individuals with an interest in soft tissue composition and dynamics.

Several error metrics, including percent variance accounted for (%VAF), were used to determine solution accuracy. Additionally, solution uncertainty was characterized using matrix conditioning and parameter covariance. The highest %VAF was observed as **82.64%** when the tissue is modelled as the HO model, but it also had the highest condition number and parameter covariance. There was a total of 45 participants who tested the models in the study. The highest percentage of individuals rated the HO model as the best. The median and mode for the KB and HO models were the highest as well, with the mode count being higher for the HO model than the KB model.

The best error metrics were from the HO black box model. However, the HO model increased the accuracy of the overall results only slightly compared to the KB model, while

having higher numerical conditioning and parameter uncertainty compared to the KB model. This means that while the HO model may have provided a better fit to the dynamic behaviour, the parameter values may be more uncertain and be easily influenced by errors in the system identification experiments. While the KB and HO models had the same median ratings, the mode count was higher for the HO model and the percentage of people who rated it the best was the highest. This may indicate that the HO model could have been preferred over the others by the study participants. Overall, the contributions of this work demonstrated that the better the model captured the dynamic behaviour of the signals, the more realistically it was perceived by the operator.

Chapter 4

Basin of Attraction Estimate for Analyzing Manual Materials Handling Tasks

4.1 Framework of Additional Study

The previous study in Chapter 3 focused on applying concepts from systems and control engineering to surgical interventions for LBP specifically in the context of MI LIF surgical simulation. However, ideally preventative measures for LBP would be utilized to delay or prevent surgical intervention. This study focuses on characterizing manual materials handling (MMH) tasks, which is relevant to the objectives of this thesis as MMH tasks impose high forces on the lower back that can lead to pain. As discussed in Chapter 2, a factor that can cause low back pain (LBP) is incorrect technique during occupational lifting. Therefore, a preventative measure for LBP could be to improve lifting techniques used in MMH tasks. Adequately characterizing lifting and depositing could provide a means of evaluating the technique used by individuals who regularly do MMH tasks and prevent occupational hazards. The depositing of MMH tasks was characterized in this study using a basin of attraction (BOA). The results from this study are preliminary and the methodology could provide a framework that could be utilized in future work. This work is presented as an alternative to existing work that evaluates stability about a static EP, as well as work that utilizes

Lyapunov exponents. The use of a basin of attraction (BOA) to quantify perturbations about a trajectory for MMH is a novel framework presented in this additional study. Ethics approval was obtained from necessary review boards (see Appendix A). This work was made in collaboration with Dr. Larièviere and retrospectively utilizes data obtained from previous studies [1, 2]. As this is preliminary work, these results are unpublished.

4.2 Additional Study: Basin of Attraction Estimate for the Analysis of Manual Materials Handling Tasks

4.2.1 Abstract

Introduction: In this work, BOAs were used to evaluate the depositing techniques of individuals performing manual materials handling. **Methods:** Two lifters were evaluated, one novice and one expert. The BOAs were determined for each subject using Lyapunov systems theory and sum of squares programming. **Results:** It was found that the novice lifter had changes in the size of their BOAs when the mass they were depositing changed. It was also found that there were differences in the size of the BOA between expert and novice lifters. **Conclusion:** These results indicated that the novice lifter may select trajectories about their centres of mass that make them more susceptible to perturbations than expert lifters. These preliminary results are limited, but could be promising for future work related to this study.

4.2.2 Introduction

Lifting tasks in MMH create high stresses on the back, making those who do occupational MMH vulnerable to chronic LBP. In particular, incorrect lifting techniques have been identified as a potential cause of LBP, resulting in occupational hazards if workers do not adopt adequate lifting strategies [3, 4]. Depositing objects with heavy masses can also cause strain on the back, which may lead to injury [5]. Spine stability is critical for the ability to bear loads

[6]. Therefore, characterizing spine stability during lifting is pertinent for preventing LBP in workers doing MMH. Previous studies have used data from expert and novice lifters to examine differences in lifting technique, with the expert lifters having differences in technique from the novice lifters [1, 2].

Spine stability has multiple definitions depending on context. The mechanical definition of stability describes how the spine and its associated systems (*e.g.*, passive and active components, and the neurological system) respond to a perturbation [7]. By this definition, the spine is considered stable when, in response to a perturbation, it is able to return to approximately the same original position [7]. If it is able to return to its exact position it is considered asymptotically stable [7]. In comparison, if it is unable to return to its original position then it is considered unstable [7]. This definition aligns with Lyapunov stability as defined in control theory [8]. As a result, the stability of the spine has been investigated about an equilibrium point using concepts from control theory. Xu *et al.* investigated optimal control strategies of the spine during an unstable seated balance task. During this task, a subject is seated on a semi-circular ball, and is subjected to a perturbation where they attempt to return to a neutral position [9]. The authors modelled this behaviour by evaluating the linear quadratic regulator (LQR) controller cost using the \mathcal{H}_2 norm [9]. While this study may have proposed a potentially effective framework for defining spine stability about equilibrium point, it did not consider stability along a trajectory. Since MMH tasks are concerned with movement along a trajectory, this framework proposed in the previous study could be improved by evaluating the movement along a trajectory instead.

Characterizing spine stability along a trajectory provides a means of modelling nonlinear system behaviour while taking into consideration dynamic effects such as inertia. Previous literature has characterized stability along a trajectory using Lyapunov exponents [10]. The Lyapunov exponents have been evaluated using repetitive tasks such as unweighted repetitive trunk movements and repetitive lifting [10–12]. The maximum Lyapunov exponent was then measured from the divergence of position, velocity, and acceleration between repetitive tasks.

A negative Lyapunov exponent indicates a system that converges to the trajectory and a positive Lyapunov exponent indicates that it diverges [10]. While the Lyapunov exponents effectively characterize divergence or convergence of the nonlinear system, they have an abstract interpretation. A method with a more intuitive interpretation in physical space may be more useful in practice.

Another way to characterize stability along a trajectory is using a basin of attraction (BOA). Intuitively, a BOA for a system represents how much the system can be perturbed and still converge to a goal region, referred to as the goal set. BOAs have been previously used to assess controller robustness and generate motion primitives for nonlinear autonomous systems [13–15]. BOAs have more recently been applied to biomechanical tasks, particularly to the sit-to-stand task [16, 17]. Holmes *et al.* validated these BOAs using cable-pull experiments to demonstrate their effectiveness for quantifying perturbations along a trajectory for the sit-to-stand task [16]. This method requires a system model to estimate the dynamics and has been used effectively with inverted pendulum models to represent centers of mass [16, 17]. Additionally, this method requires that there be a controller, with studies assuming a finite-time horizon LQR control structure [16, 17]. This is the finite-time horizon case of the controller that has previously been applied by Xu *et al.* to the spine about an equilibrium point [9]. The BOA has yet to be applied as a means of characterizing lifting strategies during MMH to quantify spine stability along a trajectory.

This work serves as a proof of concept for the use of BOAs to quantify spine stability along a trajectory during an MMH task. The objectives of this preliminary study are:

- to build a simple model for trunk movements during the depositing stage of MMH;
- to define a BOA for the trunk movements along the trajectory; and,
- to compare the BOA from a novice and an expert lifter.

The objectives were addressed by evaluating the trajectories of a novice and an expert lifter depositing a box. The subjects ($N = 2$) were modelled using a mass inverted pendulum about their centers of mass (COM). The dynamics were then controlled to the trajectory using

finite-time horizon LQR to initialize the BOA. It is hypothesized that there will be differences in the BOAs for each task and between novice lifters and expert lifters. Specifically, it is expected that novice lifters will be more susceptible to perturbations than expert lifters.

4.2.3 Methods

The data used in this study was obtained from previous studies on MMH, where subjects were expected to handle boxes of masses between 15 - 23 kg [1, 2]. The original study methods are summarized as follows. A group of male novice lifters and a group of male expert lifters were recruited based on level of experience in occupational MMH and incidence of LBP. The lifters were asked to perform MMH while wearing optical markers to study their biomechanical movement. The MMH was further subdivided into three tasks: lifting, carrying, and depositing boxes.

Leveraging the data presented in the study by Plamondon *et al.*, the additional study presented in this dissertation selected two participants, one novice and one expert lifter, for a preliminary analysis [1]. The MMH optical marker data was used to build trajectories to perform this analysis. An inverted pendulum was used to model the lifters about different centers of mass as depicted in Figure 4.1.

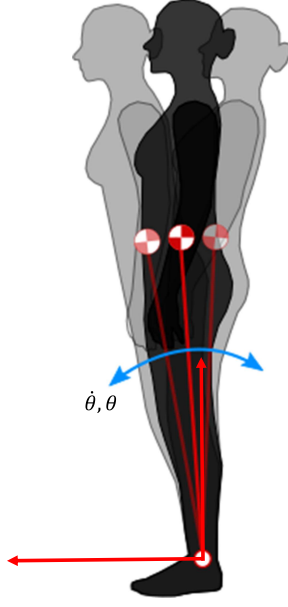


Figure 4.1: The inverted pendulum model of the total body center of mass for flexion/extension. Figure modified from [18].

The simple damped pendulum dynamics take on the form of

$$m\ell^2\ddot{\theta}(t) + b\dot{\theta}(t) + mg\ell \sin \theta(t) = u_0(t), \quad (4.1)$$

where ℓ is the length of the pendulum, m is the mass of the pendulum, b is the damping coefficient, and g is the gravitational acceleration. The length of the pendulum was determined from the average Euclidian distance along the subject's trajectory, and the mass was determined from anthropometric data and subject mass [19]. The pendulum states are then $\mathbf{x}(t) = [\theta(t) \ \dot{\theta}(t)]^T$. Formulating the BOA using the pendulum model then has the following workflow: building the state trajectory, fitting the model to the trajectories with a feedforward term and a finite-time horizon linear quadratic regulator (LQR), and computing the BOA computation.

4.2.3.1 Trajectory Generation

The trajectory was generated by calculating the COM from optical marker data. Markers were placed at different landmarks along the body with a subset of those points defining the vertices of specific segments of the torso, as in [19]. The associated masses were then calculated from subject mass weighted with anthropometric data, similar to [16, 19]. To model the torso, three centers of mass were defined: the thorax, the abdomen, and the pelvis. As shown in Figure 4.2 the thorax is between C7/T1 - T12/L1, the abdomen is between T12/L1 - L4/L5, and the pelvis is between L4/L5- the greater trochanter [19].

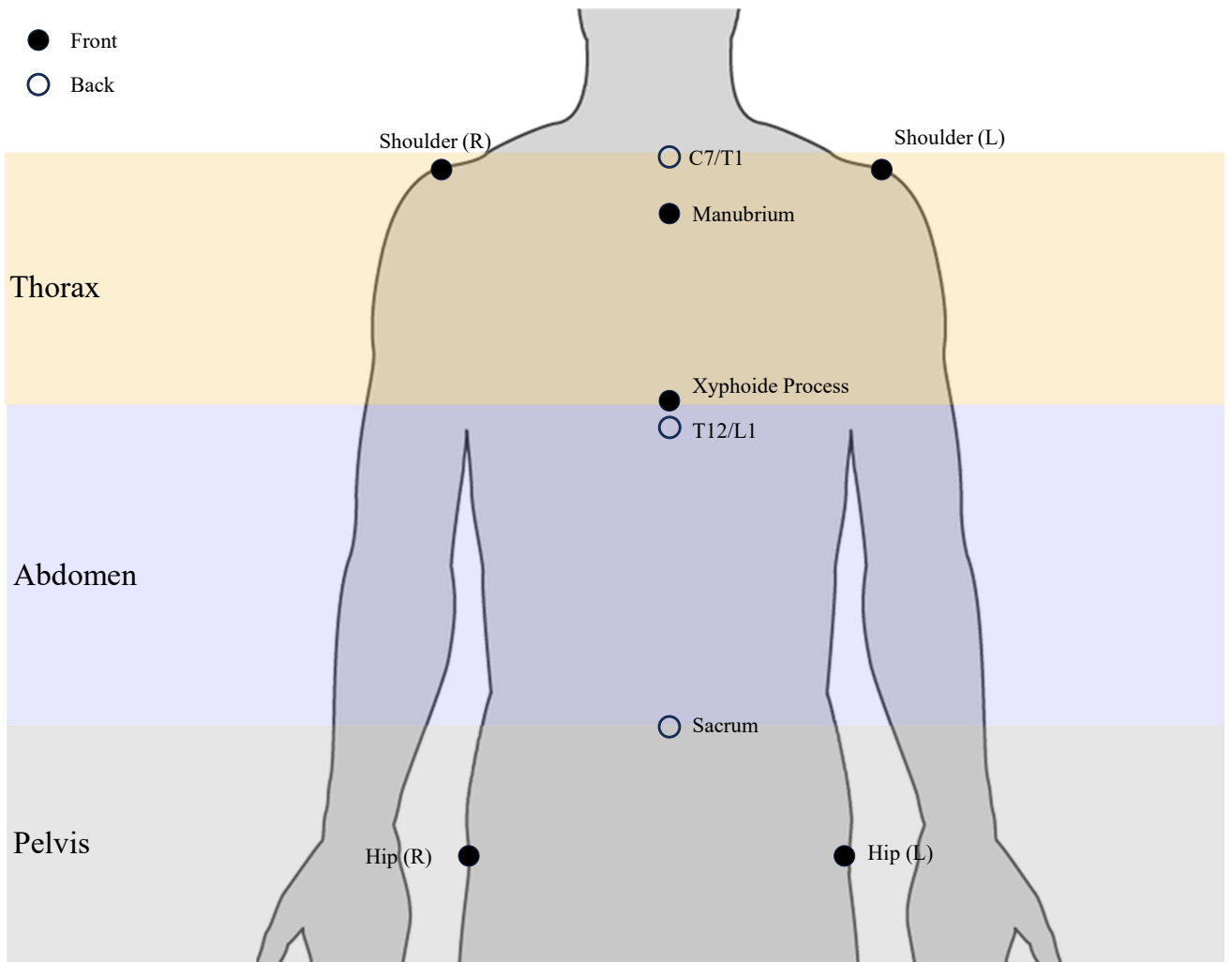


Figure 4.2: The markers on the torso and their corresponding segments: thorax, abdomen, and pelvis. Figure modified from [20].

The COM trajectories were segmented according to the three tasks in MMH: the lift, the carry, and the deposit. The end of the lifting task was segmented using the first toe off the ground and beginning of the deposit task was segmented using the minimum velocity of the wrist holding the box. The carrying task was the task between the lift and the deposit. In this study a single expert and a single novice were selected to evaluate the depositing task.

The 3D trajectories were then projected onto the xz - and yz -planes to accommodate the planar pendulum model. The trajectories were then transformed to the corresponding pendulum states of $\theta(t), \dot{\theta}(t)$ forming reference trajectories ($\mathbf{x}_0(t)$). Each trajectory was interpolated to be 1000 points using cubic spline interpolation to non-dimensionalize time. This was done to allow comparison of BOA sizes when they are the same length [16].

4.2.3.2 Feedback Controller

Once the reference trajectories ($\mathbf{x}_0(t)$) were established, a reference control input ($u_0(t)$) was built as a feedforward term using the inverse dynamics. A finite-time horizon LQR feedback controller was then calculated to adjust for deviations from the feedforward term [21]. The feedback controller was then generated using Euler integration of the differential Riccati equation (DRE) from the terminal state weighting matrix $\mathbf{S}_f = \mathbf{Q}_f$ [21]

$$-\dot{\mathbf{S}}(t) = \mathbf{Q} - \mathbf{S}(t)\mathbf{B}(t)\mathbf{R}^{-1}\mathbf{B}^T\mathbf{S}(t) + \mathbf{S}(t)\mathbf{A}(t) + \mathbf{A}^T\mathbf{S}(t), \quad (4.2)$$

where \mathbf{A} and \mathbf{B} are the time-varying linearization of the dynamics specified by

$$\begin{aligned} \bar{\mathbf{x}}(t) &= \mathbf{x}(t) - \mathbf{x}_0(t), \quad \bar{u}(t) = u(t) - u_0(t), \\ \dot{\bar{\mathbf{x}}}(t) &\approx \mathbf{A}(t)\bar{\mathbf{x}}(t) + \mathbf{B}(t)\bar{\mathbf{u}}(t). \end{aligned} \quad (4.3)$$

The \mathbf{Q} and \mathbf{R} matrices are the state weighting and control input weighting matrices, respectively. The state weighting and control input weighting matrices were tuned to both control the pendulum to the state trajectories. These matrices were also tuned to ensure that the BOA was within the same order of magnitude as the original states, as they implicitly define the goal set. They were kept the same between both subjects and their corresponding COMs.

The feedback law was then implemented as

$$\bar{u}^*(t) = -\mathbf{R}^{-1}\mathbf{B}^T(t)\mathbf{S}(t)\bar{\mathbf{x}}(t) = -\mathbf{K}(t)\bar{\mathbf{x}}(t). \quad (4.4)$$

4.2.3.3 BOA Computation

The BOA is solved using a sum of squares (SOS) optimization with free polynomial multiplier terms. One application of SOS programming is to determine whether a polynomial is positive. A positive polynomial can be given any arbitrary input, and yield a positive output [22]. In the case of this work, the search for SOS polynomials can be rewritten as a semi-definite program, which was solved using MOSEK, a commercial semi-definite program solver [23]. A feasible solution to the SOS problems provides a certificate of positivity [22]. This work was solved in Julia, in particular by using the SumOfSquares library [24, 25]. The polynomial multiplier terms (labelled as L_i in this work) are added to enforce bounded Lyapunov constraints using the generalized S-procedure. The generalized S-procedure takes on the form of

$$q(x) := p(x) - \overbrace{\sum_{i=1}^{N_{\text{eq}}} L_{\text{eq},i}(x)g_{\text{eq},i}(x) - \sum_{j=1}^{N_{\text{ineq}}} L_{\text{ineq},j}(x)g_{\text{ineq},j}(x)}^{r(x)} \text{ is SOS}, \quad (4.5)$$

$$L_{\text{ineq},j}(x) \text{ is SOS}, \forall j \in \{0, \dots, N_{\text{ineq}}\}$$

where $L_{\text{eq},i}(x)$ and $L_{\text{ineq},j}(x)$ are free polynomial terms that exist to modify polynomial equalities and inequalities. When the equalities and inequalities are $g_{\text{eq},i}(x) = 0$ and $g_{\text{ineq},i}(x) \geq 0$, it implies that for the $q(x)$ to be SOS, $p(x)$ must be positive since $r(x)$ is negative [14, 22]. The generalized S-procedure thereby allows additional nonnegativity constraints to be incorporated into the SOS program. The BOA can then be computed using the following

optimization problem, obtained from [13–15]

$$\begin{aligned} & \underset{\rho(t_i), L_i(\bar{x})}{\text{maximize}} \sum_{i=1}^N \rho(t_i) \\ & \text{subject to } -\dot{V}_i(\bar{x}) + \dot{\rho}(t_i) + L_i(\bar{x})(V_i(\bar{x}) - \rho(t_i)) \text{ is SOS.} \end{aligned} \quad (4.6)$$

This optimization problem scales the bounds of the invariant set approximated by the solution to the DRE at each timestep by a coefficient ρ , as \mathbf{S}_i/ρ_i . The optimization is non-convex, so it was solved as a bilinear alternation problem. The bilinear alternation problem starts by finding a feasible polynomial multiplier for each point along the trajectory. This is done by solving equation (4.6) with fixed values for $\rho(t)$. The $\rho(t_i)$ is decreased as a geometric progression until a feasible solution is returned [26]. Then the maximization is solved for each feasible point, with the modified $\rho(t_i)$ from the geometric progression to approximate $\dot{\rho}$ and the feasible L_i . For both steps V_i is defined as

$$V_i(t, \bar{\mathbf{x}}) = (\mathbf{x} - \mathbf{x}_0(t))^T \mathbf{S}(t) (\mathbf{x} - \mathbf{x}_0(t)) = \bar{\mathbf{x}}^T \mathbf{S}(t) \bar{\mathbf{x}}, \quad (4.7)$$

where $\mathbf{S}(t)$ can be found by solving equation 4.2 [13–15, 21].

4.2.4 Results

The solution from the finite-time horizon LQR was expanded using the SOS bilinear alternation to produce Figure 4.3 for the abdomen COM of an expert lifter. The BOA in Figure 4.3 expands away from the goal set, while staying within the order of magnitude of the initial solution. For each subject, and each COM, the solution was produced across 1000 points using two alternations of feasible expansion points [15]. The output of the optimization is a $\rho(t)$ that can scale the solutions to Equation 4.2

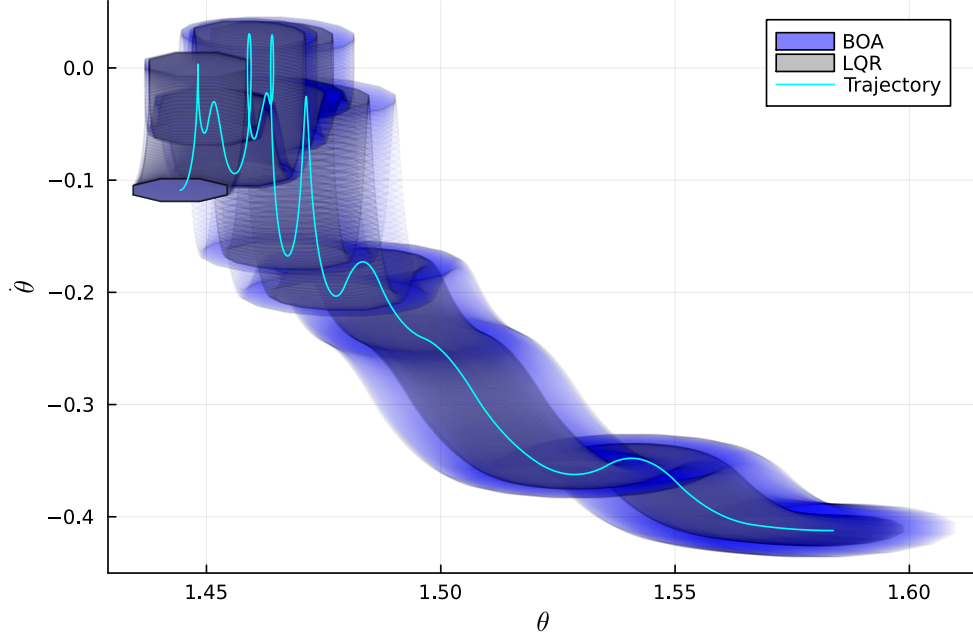


Figure 4.3: Finite-time horizon LQR solution with expanded BOA over the abdomen COM trajectory projected onto $\theta, \dot{\theta}$.

The trajectories were projected onto the yz -plane (flexion/extension) and the xz -plane (lateral bending) then transformed to the $\theta, \dot{\theta}$ region of state space. For the expert and novice lifters the BOA was determined for the depositing task in flexion/extension and lateral bending. The remaining BOAs from the expert subject are shown in Figure 4.4.

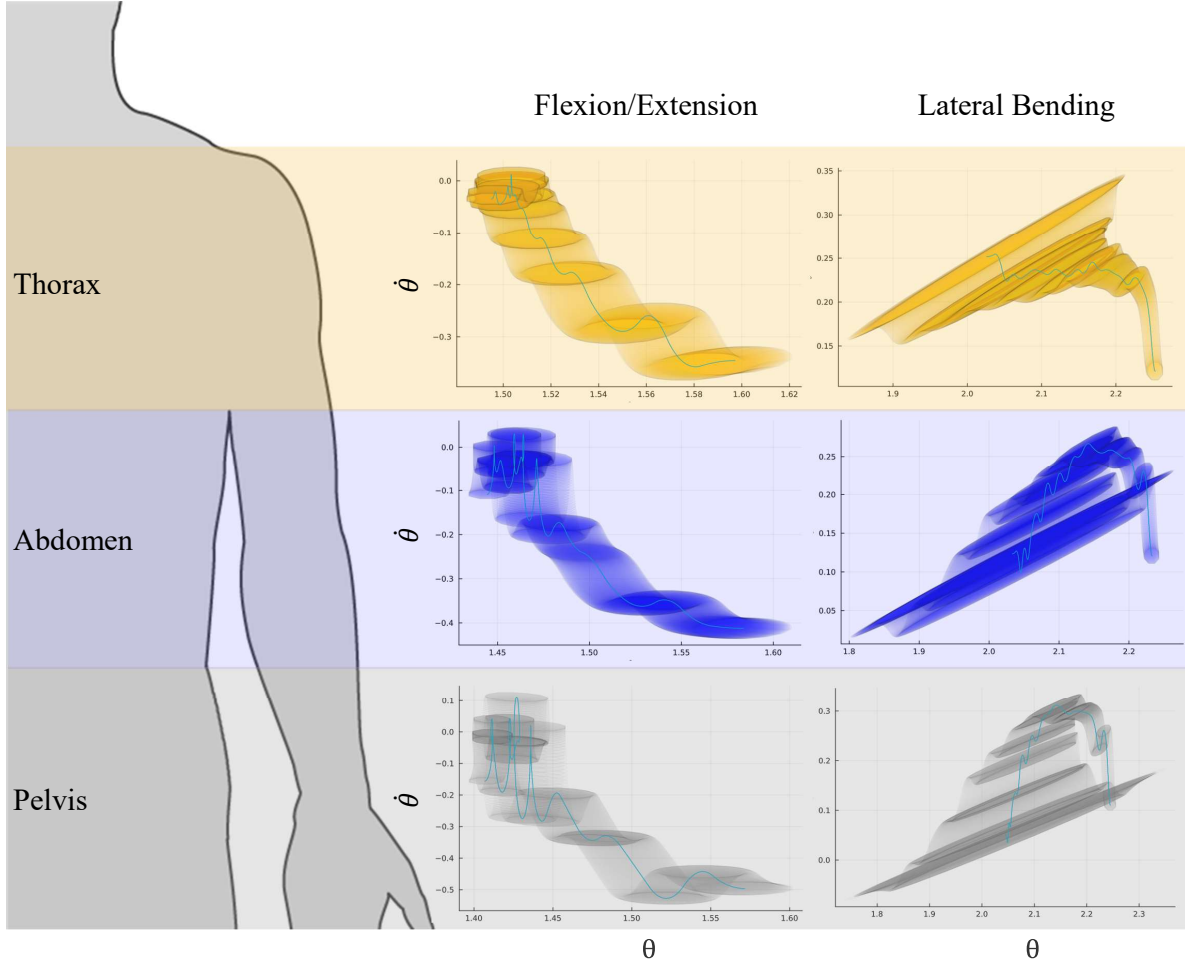


Figure 4.4: BOA around trajectories of each COM of an expert lifter: thorax, abdomen, pelvis. BOAs are projected onto the $\theta, \dot{\theta}$ region of state space. Figure modified from [20]

The average BOA cross-section was determined for each COM for both the novice lifter and the expert lifter. The percent difference of the average cross-sectional area was determined between an experienced lifter and novice lifter. The percent difference was also found for each experience-level when the mass of the box was decreased from 23 kg to 15 kg. The results of the percent differences are presented in Table 4.1.

Table 4.1: Percent difference in average cross-sectional area of the basin of attraction for each COM, in the depositing task, between an expert and novice, and for a decrease in mass (DM) from 23 kg to 15 kg

	COM	Lateral Bending (%)	Flexion/Extension (%)
Expert and Novice	Thorax	2.27	-0.02
	Abdomen	2.92	-0.09
	Pelvis	4.44	-0.81
DM: Expert	Thorax	0.04	0.07
	Abdomen	-0.07	-0.10
	Pelvis	-0.87	-0.13
DM: Novice	Thorax	1.19	-0.51
	Abdomen	5.02	-1.55
	Pelvis	7.51	-2.84

4.2.5 Discussion

This study examined three COM trajectories during the depositing stage of an MMH task. The hypothesis was that novice lifter will select trajectories about their COMs that are more susceptible to perturbations than the expert lifter. As this is a preliminary study, subjects ($N = 2$) were modelled using a simple mass inverted pendulum. The mass was defined at their thoracic, abdominal, and pelvic COMs. The finite-time horizon LQR was then used to fit the dynamics to the depositing trajectories, and the solution provided an initial guess for the BOA computation. From the results, a feasible ρ was obtained that expanded the finite-time LQR solution at each point from the initial conditions to the goal set. In Figure 4.3, the BOA expanded within the order of magnitude of the initial guess and the trajectory states, demonstrating a potentially reasonable solution to the expansion.

The average cross-sectional areas (aCSA) of the BOAs were then evaluated to determine the differences between the novice and expert lifters, and the response to different masses that were used in the depositing task. A BOA is defined by a terminal goal, in this case, that represents the region where the box is deposited. A larger BOA indicates that the subject can be perturbed more while still being able to reach the terminal goal, while a smaller

BOA indicated that a subject can be perturbed less. The percent differences between aCSAs are summarized in Table 4.1. The largest differences in the aCSAs was observed in lateral bending. In particular, the aCSAs were larger for the expert than the novice, with the percent difference being as much as 4.44% in the pelvic COM. This indicates that the expert during the depositing task could withstand larger perturbations than the novice on average along the trajectory. Additionally, decreasing mass lead to almost no change in the aCSA of the BOA for the expert, but a larger change in that of the novice particularly in lateral bending. In this case, the aCSA increased upon a decrease in mass, with up to a 7.51% increase in size. This indicates that the novices may be more susceptible to changes in mass than the expert lifters.

While these preliminary results are promising, they have several limitations. The system dynamics are under-constrained, which could be constrained further through more rigorous experimentation and system identification. The mass inverted pendulum models are simple compared to existing models of regions of the torso, which could be leveraged in future studies [27]. A model that depends on states in physical space, instead of phase space, would provide a more intuitive representation of the BOA as well, as has been done with other autonomous systems [14]. Some dynamics may also be lost when using a planar pendulum, model, so extending the model to three dimensions could capture more system behaviour as well. The parameters of the finite-time horizon LQR were also tuned to the problem, although using a controller that is identified from the data could provide a more realistic representation of the controller inherent to the subject [28]. Additionally, actuator limits could also be determined experimentally based on limitations of human movement during the task and integrated into the cost function to further constrain the problem [14]. Actuator limits and improved models would provide a more realistic representation of the closed-loop system. Moreover, this additional study used a small sample size, so increasing the number of participants could provide statistical measurements of uncertainty and significance to draw conclusions from. Finally, while the SOS programs certify that the BOAs form invariant sets around

the trajectories, additional validation studies could be performed in future work. Studies similar to the cable-pull experiments by Holmes *et al.*, which perturbed subjects along their trajectories would validate the use of BOAs to measure stability [16]. The BOAs could also be validated numerically in future studies using Monte Carlo simulations to ensure that they are adequately capturing the trajectories that converge to the goal and to test the sensitivity of different model assumptions. Overall, the preliminary results demonstrate potential but, with additional work, a more comprehensive definition of the BOA for the trunk could be defined.

4.2.6 Conclusion

In conclusion, this preliminary study demonstrated a successful implementation of BOAs for evaluating the stability of trunk COMs along a trajectory. While there are limitations that leave many opportunities for future work, the results demonstrate that there are potentially differences in BOA shape depending on the expertise of the lifter.

4.2.7 References

- [1] A. Plamondon, C. Larivière, A. Delisle, D. Denis, and D. Gagnon, “Relative importance of expertise, lifting height and weight lifted on posture and lumbar external loading during a transfer task in manual material handling”, *Ergonomics*, vol. 55, no. 1, pp. 87–102, 2012.
- [2] D. Gagnon, N. Arjmand, A. Plamondon, A. Shirazi-Adl, and C. Larivière, “An improved multi-joint emg-assisted optimization approach to estimate joint and muscle forces in a musculoskeletal model of the lumbar spine”, *Journal of biomechanics*, vol. 44, no. 8, pp. 1521–1529, 2011.
- [3] D. B. Chaffin and K. S. PARK, “A longitudinal study of low-back pain as associated with occupational weight lifting factors”, *American Industrial Hygiene Association Journal*, vol. 34, no. 12, pp. 513–525, 1973.

- [4] S. M. Hsiang, G. E. Brogmus, and T. K. Courtney, “Low back pain (lbp) and lifting technique—a review”, *International Journal of Industrial Ergonomics*, vol. 19, no. 1, pp. 59–74, 1997.
- [5] S. A. Ferguson *et al.*, “Prevalence of low back pain, seeking medical care, and lost time due to low back pain among manual material handling workers in the united states”, *BMC musculoskeletal disorders*, vol. 20, no. 1, pp. 1–8, 2019.
- [6] M. M. Panjabi *et al.*, “The stabilizing system of the spine. part i. function, dysfunction, adaptation, and enhancement”, *Journal of spinal disorders*, vol. 5, pp. 383–383, 1992.
- [7] N. P. Reeves, K. S. Narendra, and J. Cholewicki, “Spine stability: The six blind men and the elephant”, *Clinical biomechanics*, vol. 22, no. 3, pp. 266–274, 2007.
- [8] H. K. Khalil, *Nonlinear systems*. Prentice Hall, 2002.
- [9] Y. Xu, J. Choi, N. P. Reeves, and J. Cholewicki, “Optimal control of the spine system”, 2010.
- [10] K. Granata and P. Gottipati, “Fatigue influences the dynamic stability of the torso”, *Ergonomics*, vol. 51, no. 8, pp. 1258–1271, 2008.
- [11] R. B. Graham, E. M. Sadler, and J. M. Stevenson, “Does the personal lift-assist device affect the local dynamic stability of the spine during lifting?”, *Journal of biomechanics*, vol. 44, no. 3, pp. 461–466, 2011.
- [12] R. B. Graham and S. H. Brown, “A direct comparison of spine rotational stiffness and dynamic spine stability during repetitive lifting tasks”, *Journal of biomechanics*, vol. 45, no. 9, pp. 1593–1600, 2012.
- [13] A. Majumdar, A. A. Ahmadi, and R. Tedrake, “Control design along trajectories with sums of squares programming”, in *2013 IEEE International Conference on Robotics and Automation*, IEEE, 2013, pp. 4054–4061.

- [14] A. Majumdar and R. Tedrake, “Funnel libraries for real-time robust feedback motion planning”, *The International Journal of Robotics Research*, vol. 36, no. 8, pp. 947–982, 2017.
- [15] M. M. Tobenkin, I. R. Manchester, and R. Tedrake, “Invariant funnels around trajectories using sum-of-squares programming”, *IFAC Proceedings Volumes*, vol. 44, no. 1, pp. 9218–9223, 2011.
- [16] P. D. Holmes, S. M. Danforth, X.-Y. Fu, T. Y. Moore, and R. Vasudevan, “Characterizing the limits of human stability during motion: Perturbative experiment validates a model-based approach for the sit-to-stand task”, *Royal Society open science*, vol. 7, no. 1, p. 191 410, 2020.
- [17] V. Shia, T. Y. Moore, P. Holmes, R. Bajcsy, and R. Vasudevan, “Stability basin estimates fall risk from observed kinematics, demonstrated on the sit-to-stand task”, *Journal of biomechanics*, vol. 72, pp. 37–45, 2018.
- [18] *File:inverted pendulum human balance.png*, Date obtained: July 25, 2023. [Online]. Available: https://commons.wikimedia.org/wiki/File:Inverted_Pendulum_Human_Balance.png#.
- [19] D. A. Winter, *Biomechanics and motor control of human movement*. John wiley & sons, 2009.
- [20] *File:people - outlines - smart-servier.png*, Date obtained: July 19, 2023. [Online]. Available: https://commons.wikimedia.org/wiki/File:People_-_Outlines_-_Smart-Servier.png.
- [21] R. Tedrake, I. R. Manchester, M. Tobenkin, and J. W. Roberts, “Lqr-trees: Feedback motion planning via sums-of-squares verification”, *The International Journal of Robotics Research*, vol. 29, no. 8, pp. 1038–1052, 2010.
- [22] P. A. Parrilo, *Structured semidefinite programs and semialgebraic geometry methods in robustness and optimization*. California Institute of Technology, 2000.

- [23] M. ApS, *<https://docs.mosek.com/latest/capi/index.html>*, 2022. [Online]. Available: <https://docs.mosek.com/latest/capi/index.html>.
- [24] B. Legat, C. Coey, R. Deits, J. Huchette, and A. Perry, “Sum-of-squares optimization in Julia”, in *The First Annual JuMP-dev Workshop*, 2017.
- [25] T. Weisser, B. Legat, C. Coey, L. Kapelevich, and J. P. Vielma, “Polynomial and moment optimization in julia and jump”, in *JuliaCon*, 2019. [Online]. Available: <https://pretalx.com/juliacon2019/talk/QZBKAU/>.
- [26] F. Girlanda, *Sos-bilinear-alternation*, GitHub repository, 2022. [Online]. Available: <https://github.com/FedericoGirlanda/SOS-bilinear-alternation>.
- [27] I. El Bojairami, K. El-Monajjed, and M. Driscoll, “Development and validation of a timely and representative finite element human spine model for biomechanical simulations”, *Scientific Reports*, vol. 10, no. 1, p. 21 519, 2020.
- [28] P. Van Overschee and B. De Moor, “Closed loop subspace system identification”, in *Proceedings of the 36th IEEE Conference on Decision and Control*, IEEE, vol. 2, 1997, pp. 1848–1853.

Chapter 5

Discussion

The spine is a system that relies on multiple structures to maintain stability and mitigate pain. Low back pain (LBP) can occur from a variety of factors including degenerative diseases of the spine and environmental and genetic factors. LBP is a leading cause of disability and workplace absence, and being able to prevent or alleviate LBP is an active area of research. LBP can be prevented by mitigating environmental factors that lead to pain and encourage a healthy spine. In the event that preventative measures are not effective, then surgical intervention is often prescribed to minimize the major symptoms associated with LBP.

Surgical intervention of LBP often takes the form of a minimally invasive (MI) lumbar interbody fusion (LIF) procedure. However, surgical errors can lead to complications during treatment that can cause longterm harm to the patient[25, 26]. High-fidelity simulators use realistic tissue force feedback when the surgeon is first gaining access to the target structure for surgery. During this time, the surgeon receives almost no visual cues and relies on the tactile feedback from the soft tissue. A high-fidelity surgical simulation platform that provides comprehensive surgical training can help reduce complications from difficult steps in the LIF procedures.

Preventative measures can be improved by by determining comprehensive evaluation metrics for activities with a high likelihood of causing LBP. One such activity is manual materials handling (MMH), which when done with incorrect technique, has a high incidence of LBP [20]. MMH can be characterized in terms of the lifting trajectories. This is different

from other biomechanical tasks, such as the unstable seated balance task, which are concerned with spine stability about a static EP [96].

Techniques adopted from systems and control engineering can be leveraged to model the dynamics that govern the spine during lifting, and the tissues appended to the spine that are navigated during surgical treatment. These techniques from systems and control engineering were leveraged in this thesis and resulted in the following novel contributions to the research field:

- **Chapter 3:** dynamic soft tissue models of the spine were developed using system identification (ID) and were implemented in a LIF surgical simulator. The novel contribution of this study was using and validating dynamic models and signals to represent the force feedback dynamics of soft tissues in a spine LIF surgical simulator. To the author's knowledge, this is the first study to provide a framework for this procedure that utilizes both dynamic signals and dynamic models for this procedure.
- **Chapter 4:** the stability of trunk movements for MMH tasks along a trajectory were examined using a basin of attraction (BOA). The novel contribution of this additional study was that it provided a framework for characterizing dynamic stability of trunk movements during MMH tasks using BOAs. To the author's knowledge, this is the first application of BOAs to characterize the MMH task.

The specific objectives addressed in the studies presented in this thesis are summarized in Table 5.1. The discussion on methodologies and limitations related to those objectives are described in Chapters 3 and 4. Beyond the specific objectives, both studies exploited dynamics and optimization to characterize systems related to the spine. In the first manuscript, this was accomplished by identifying dynamic viscoelastic models with least squares optimization. In the additional study, this was accomplished using SOS programming to define a BOA about a trajectory. The topics of dynamics, numerical computing, and optimization were discussed with reviewers of the first manuscript, and were integral to both works. These topics are further elaborated on below.

Table 5.1: Objectives addressed in this thesis. The manuscript explored modelling of spine soft tissue force feedback while the additional study modelled trunk stability along a trajectory.

Modelling spine tissue force feedback	Modelling trunk stability along a trajectory
<ul style="list-style-type: none"> • to identify the tissue force feedback response as the dynamic systems outlined in Figure 3.2 and, • to examine the tradeoff between the accuracy of the force feedback models with respect to the tissue dynamic behaviour, and how the models are rated by the operator when programmed into a surgical simulator. 	<ul style="list-style-type: none"> • build a simple model for trunk movements during the depositing stage of MMH, • define a BOA for the trunk movements along the trajectory and, • compare the BOA from a novice and an expert lifter.

Modelling system dynamics is an important component of both works showcased in this thesis, as dynamics play a key role in describing many systems. Thus, techniques from systems and control engineering are often focused on characterizing a system’s dynamics. The first manuscript is concerned with exploiting the property of viscoelasticity to identify soft tissue force feedback models. The system identification procedure performed in the first manuscript inherently identifies dynamic models. Since the identified models had components that depend on time, and thus frequency, they can be categorized as dynamic models. Additionally, the input signals used to identify these models were designed to excite the tissue analogue across a bandwidth of frequencies to capture the behaviour of the frequency-dependent components of the model. This was presented as an alternative to procedures in surgical simulation and surgical robotics that do not identify dynamic models and identification procedures that use static signals [56, 57, 97]. The additional study presented in this thesis is concerned with dynamics as well. Spine stability is often characterized in terms of a static equilibrium point [77, 96]. However, this work presents a novel way of characterizing trunk movements along a trajectory using a BOA. Quantifying trunk movements in terms of perturbations along a trajectory provides a novel way of representing MMH tasks that could not be done similarly about a static equilibrium.

In addition to dynamics, both of the studies presented in this thesis exploit optimization and numerical computing techniques. Despite many recent efforts in imaging and medical technology, many behaviours of the human body cannot be easily observed [77]. Work in systems and control theory implement optimization procedures to generate models and characterize systems from data. In this work, optimization and numerical computing provided a means to determine information from data that is otherwise not easily determined through experimentation alone. In the first study, system identification was employed to model the complex interaction dynamics between the surgeon and soft tissue that results in force feedback. System identification was able to capture the interaction dynamics by utilizing least squares optimization to build dynamic system models. The viscoelastic parameters of materials can be determined purely experimentally through several material testing procedures [98]. However, the methodologies of this study were designed to model the dynamics of the access-gaining step of the surgery specifically. The tool tip feedback during the surgery is not simply a function of the viscoelasticity, but also includes material fracture, deformation, and friction which are difficult to determine from mechanical testing alone [99]. Adjustments to the identification cost function were made to incorporate Tikhonov regularization, which encourages system stability and numerical conditioning. Hyperparameter optimization was used to identify the weight of regularization term. Regularization was particularly important for the higher order (HO) model which was a fourth order biproper transfer function, as it helped improve the numerical conditioning for the higher number of force and system elements. Therefore, least squares and corresponding regularization techniques played an integral role in adequately modelling the force feedback dynamics of the soft tissue. In the additional study, BOAs were used as means of assessing the trunk's response to perturbations along a trajectory. Perturbations about an equilibrium point (EP) have been measured for postural sway about a person's COM using only data obtained from experiments, called a cone of economy [100]. The cone of economy has been clinically relevant for demonstrating sway about an EP, but not for perturbations along a trajectory [101]. Additionally, stability along

a trajectory has been quantified from experimental data, without implementing optimization procedures, using Lyapunov exponents [82]. However, the Lyapunov exponents also do not give an indication to how much an individual can be perturbed along the trajectory, they measure the rate of separation between closely diverging trajectories. Quantifying the extent to which an individual can be perturbed along a trajectory can thus not be easily obtained from experimental data without leveraging optimization. The use of Sum of squares (SOS) programming plays a large role in the ability to create BOAs. SOS programming provides a means of certifying polynomial positivity through semidefinite programming [85]. This can be applied to searching for Lyapunov functions parameterized as sum-of-squares polynomials [85]. Therefore, utilizing SOS tools was important in this work to reveal information from trajectory and subject data. In conclusion, while experiments and imaging in biomechanical research provide valuable insight into how the human body behaves, numerical optimization tools can provide information that cannot be easily observed using raw data alone.

5.1 Future Work

There were several limitations from the studies outlined in this thesis. The limitations regarding the specific objectives and methodologies in the study are described in Chapters 3 and 4. However, the broad limitations of this work are from modelling real systems, and assumptions are made in both the first and additional study to accommodate the study objectives. In the first study, the force feedback was assumed to act in only a single direction. This assumption was made to keep movements between study participants consistent. However, tissue force feedback occurs in all degrees of freedom in physical space. In the additional study, an inverted pendulum was used to model the subject's COM. This assumption was made to obtain preliminary results and further validation is needed before scaling up the number of model states.

Both study methodologies have limitations on how many components can be included in the models. In the first study, there was a tradeoff between how many elements were

in the tissue force feedback models, and how well conditioned the system was. Eventually, the accuracy obtained from higher model complexity was outweighed by the high model uncertainty. In the additional study, there was a tradeoff between the number of system states and the computational complexity of the SOS program. Thus, the more system states that are considered, the longer the computational time. In general, it is not possible to model a real system without assumptions, which is particularly true for high-dimensional nonlinear systems such as human beings. A model may not capture every possible component of the human body, but instead can be simplified to consider only what is necessary for its application. Therefore, it is important to validate models adequately within the context that it is used and scale the model complexity appropriately to the problem.

There are multiple avenues that can be pursued to expand the fidelity of this work and validate proposed methodologies in future studies. The following are suggestions for future work to extend beyond what is presented in this thesis:

- Models presented in the first study could be extended to more degrees of freedom to capture the surgeons movement in higher dimensions and model the anisotropic properties of tissue.
- Models in the first study could be determined from organic simulators such as cadavers or animal models.
- The model in the additional study could be made more representative of the behaviour from humans than an inverted pendulum such as by using a finite element model.
- Models in the first study could be trained at different frequencies to investigate the role of haptic interaction rate on the stiffness and model fidelity.
- The model in the additional study could be further constrained with additional data on MMH.
- The BOA procedure could be validated with perturbation tests on human subjects performing MMH tasks.
- The BOA in the additional study could incorporate system identification to identify a controller from a spine model for the nonlinear closed loop system.

Chapter 6

Conclusion

The work in this thesis applied concepts from system and control engineering to surgical interventions and preventative measures for low back pain (LBP). The literature review in Chapter 2 motivated the objectives and discussed the pertinent background and state of the art. Specifically, anatomy and physiology of the spine and underlying mechanisms of LBP, surgical intervention of LBP in the context of surgical simulation, and preventative measures in the context of characterizing tasks that may cause LBP were discussed in the literature review. The subsequent objectives were to develop dynamic soft tissue force feedback models for a lumbar interbody fusion (LIF) surgical simulation, and to develop estimates for a BOA to evaluate MMH tasks.

Chapter 3 presented the study related to surgical simulation. In this study, tissue force feedback was treated as a dynamic system. Classical system ID was performed on a tissue analogue across a bandwidth of frequencies, the input and output signals were fit with dynamic viscoelastic models with a varying number of springs and dampers. The viscoelastic models were then integrated into a haptic device and evaluated by clinical professionals. It was found that the closer the dynamic model was to the dynamic signals, the more favoured it was by the operator, thus demonstrating the potential need for considering tissue dynamics.

Chapter 4 presented a preliminary study related to characterizing lifting technique. An expert and a novice lifter were tracked with markers during a lifting task. The center of mass (COM) of their trunk segments were determined from anthropometric data and modelled as

a simple pendulum. The BOAs were then built using SOS programming with constraints based on Lyapunov's direct method. Differences in the average cross-sectional area of the BOAs were found for each lifter. The results demonstrated that the expert and novice lifters had differences in their average cross-sectional area such that the novice lifter may select trajectories about their COMs that make them more susceptible to perturbations than the expert lifter. This was a preliminary study and therefore has many limitations, but the results lay the groundwork for future studies.

The objectives are therefore satisfied in Chapters 3 and 4. The implications, limitations, and opportunities for future work are then elaborated on in Chapter 5. In this chapter, the role of dynamics, optimization, and numerical computing are discussed in connection to both studies. Future research can expand the complexity of this work using more advanced models and by establishing rigorous experimental validation procedures.

In conclusion, this thesis provided two novel contributions by applying concepts from system and control engineering to spine biomechanics. Firstly, this work used and validated dynamic models and signals to represent the force feedback dynamics of soft tissues in a spine LIF surgical simulator. Secondly, this work provided a framework for characterizing dynamic stability of trunk movements during MMH tasks using BOAs.

Appendices

Appendix A

Ethics Approvals



McGill

Faculty of
Medicine and
Health Sciences

Faculté de
médecine et des
sciences de la santé

3655 Sir William Osler #633
Montreal, Quebec H3G 1Y6

3655, Promenade Sir William Osler #633
Montréal (Québec) H3G 1Y6

Tél/Tel: (514) 398-3124

23 August 2022

Prof. Mark Driscoll
Department of Mechanical Engineering
MacDonald Engineering Building
817 Sherbrooke Street West, Room 270
Montreal QC H3A 0C3

RE: IRB Study Number A03-M15-20A / eRAP 20-03-019

The development and evolution of a novel surgical spine procedure into a physics driven virtual reality FEM training platform

Dear Prof. Driscoll,

On 22 August 2022, at a meeting of the McGill Institutional Review Board, the following amendment received a full Board review and approval:

- Amendment Notification and Summary dated 09 August 2022
- Amended Study Protocol (August 2022)
- Participant Informed Consent Form, version 22 August 2022.

Investigators are reminded of the requirement to report all McGill IRB approved study documents to the Research Ethics Offices (REOs) of participating study sites, if applicable. Please contact the individual REOs for instructions on how to proceed. Research funds may be withheld and/or the study's data may be revoked if there is a failure to comply with this requirement.

Sincerely,

Roberta Palmour, PhD
Chair
Institutional Review Board

Cc: A03-M15-20A / 20-03-019

Figure A.1: Ethics approval for work in Chapter 3



CERTIFICATE OF ETHICS APPROVAL

REB File Number: 23-01-064
Project Title: Reachability Analysis of Manual Materials Handling Tasks
Faculty Principal Investigator: Mark Driscoll
Department: Mechanical Engineering
Sponsor/Funding Agency (if applicable): .
Research Team (if applicable):

Name	Affiliation
------	-------------

Approval Period:

FROM

16-Feb-2023

TO

15-Feb-2024

The *REB-1* reviewed and approved this project by Delegated review in accordance with the requirements of the McGill University Policy on the Ethical Conduct of Research Involving Human Participants and the Tri-Council Policy Statement: Ethical Conduct For Research Involving Humans.

- * Approval is granted only for the research and purposes described.
- * The PI must inform the REB if there is a termination or interruption of their affiliation with the University. The McGill REB approval is no longer valid once the PI is no longer a student or employee.
- * An **Amendment** form must be used to submit any proposed modifications to the approved research. Modifications to the approved research must be reviewed and approved by the REB before they can be implemented. Changes to funding or adding new funding to a previously unfunded study must be submitted as an Amendment.
- * A **Continuing Review** form must be submitted before the above expiry date. Research cannot be conducted without a current ethics approval. Submit 2-3 weeks ahead of the expiry date.
- A total of 5 renewals are permitted after which time a new application will need to be submitted.
- * A **Termination** form must be submitted to inform the REB when a project has been completed or terminated.
- * A **Reportable New Information** form must be submitted to report any unanticipated issues that may increase the risk level to participants or that may have other ethical implications or to report any protocol deviations that did not receive prior REB approval.
- * The REB must be promptly notified of any new information that may affect the welfare or consent of participants.
- * The REB must be notified of any suspension or cancellation imposed by a funding agency or regulatory body that is related to this study.
- * The REB must be notified of any findings that may have ethical implications or may affect the decision of the REB.

Figure A.2: Ethics approval for work in Chapter 4

References

- [1] H. Singh, G. C. Chang Chien, and R. Bolash, “Anatomy of the spine”, *Treatment of Chronic Pain Conditions: A Comprehensive Handbook*, pp. 11–20, 2017.
- [2] T. R. Oxland, “Fundamental biomechanics of the spine—what we have learned in the past 25 years and future directions”, *Journal of biomechanics*, vol. 49, no. 6, pp. 817–832, 2016.
- [3] *File:gray 111 - vertebral column-coloured.png*, Date obtained: July 22, 2023. [Online]. Available: https://commons.wikimedia.org/wiki/File:Gray_111_-_Vertebral_column-coloured.png.
- [4] G. Cramer, “General characteristics of the spine. cramer gd, darby sa, basic and clinical anatomy of the spine”, *Spinal Cord and ANS. 2nd Ed, Missouri: Mosby*, pp. 18–69, 2005.
- [5] M. Humzah and R. Soames, “Human intervertebral disc: Structure and function”, *The Anatomical Record*, vol. 220, no. 4, pp. 337–356, 1988.
- [6] N. Inoue and A. A. E. Orías, “Biomechanics of intervertebral disk degeneration”, *Orthopedic Clinics*, vol. 42, no. 4, pp. 487–499, 2011.
- [7] A. Nachemson, “Lumbar intradiscal pressure: Experimental studies on post-mortem material”, *Acta Orthopaedica Scandinavica*, vol. 31, no. sup43, pp. 1–104, 1960.
- [8] *File:716 intervertebral disk.svg*, Date obtained: July 21, 2023. [Online]. Available: https://commons.wikimedia.org/wiki/File:716_Intervertebral_Disk.svg.
- [9] B. Zazulak, J. Cholewicki, and P. N. Reeves, “Neuromuscular control of trunk stability: Clinical implications for sports injury prevention”, *JAAOS-Journal of the American Academy of Orthopaedic Surgeons*, vol. 16, no. 9, pp. 497–505, 2008.
- [10] H. D. Dave, M. Shook, and M. Varacallo, “Anatomy, skeletal muscle”, 2019.
- [11] R. Izzo, G. Guarnieri, G. Guglielmi, and M. Muto, “Biomechanics of the spine. part i: Spinal stability”, *European journal of radiology*, vol. 82, no. 1, pp. 118–126, 2013.
- [12] B. Henson, B. Kadiyala, and M. A. Edens, “Anatomy, back, muscles”, 2019.
- [13] N. Bogduk, M. Percy, and G. Hadfield, “Anatomy and biomechanics of psoas major”, *Clinical Biomechanics*, vol. 7, no. 2, pp. 109–119, 1992.

- [14] G. Bell, O. Dunbar, J. Beck, and A. Gibb, “Variations in strength of vertebrae with age and their relation to osteoporosis”, *Calcified tissue research*, vol. 1, pp. 75–86, 1967.
- [15] L. Lidgren, *The bone and joint decade 2000-2010*, 2003.
- [16] D. Hoy, P. Brooks, F. Blyth, and R. Buchbinder, “The epidemiology of low back pain”, *Best practice & research Clinical rheumatology*, vol. 24, no. 6, pp. 769–781, 2010.
- [17] B. W. Koes, M. Van Tulder, and S. Thomas, “Diagnosis and treatment of low back pain”, *Bmj*, vol. 332, no. 7555, pp. 1430–1434, 2006.
- [18] S. P. Cohen, C. E. Argoff, and E. J. Carragee, “Management of low back pain”, *Bmj*, vol. 337, 2008.
- [19] D. B. Chaffin and K. S. PARK, “A longitudinal study of low-back pain as associated with occupational weight lifting factors”, *American Industrial Hygiene Association Journal*, vol. 34, no. 12, pp. 513–525, 1973.
- [20] S. M. Hsiang, G. E. Brogmus, and T. K. Courtney, “Low back pain (lbp) and lifting technique—a review”, *International Journal of Industrial Ergonomics*, vol. 19, no. 1, pp. 59–74, 1997.
- [21] Y.-S. Choi, “Pathophysiology of degenerative disc disease”, *Asian spine journal*, vol. 3, no. 1, p. 39, 2009.
- [22] R. J. Mobbs, K. Phan, G. Malham, K. Seex, and P. J. Rao, “Lumbar interbody fusion: Techniques, indications and comparison of interbody fusion options including plif, tlif, mi-tlif, olif/atp, llif and alif”, *Journal of spine surgery*, vol. 1, no. 1, p. 2, 2015.
- [23] M. G. Kaiser *et al.*, “Guideline update for the performance of fusion procedures for degenerative disease of the lumbar spine. part 1: Introduction and methodology”, *Journal of Neurosurgery: Spine*, vol. 21, no. 1, pp. 2–6, 2014.
- [24] J. C. Eck, S. Hodges, and S. C. Humphreys, “Minimally invasive lumbar spinal fusion”, *JAAOS-Journal of the American Academy of Orthopaedic Surgeons*, vol. 15, no. 6, pp. 321–329, 2007.
- [25] M. Panagioti *et al.*, “Prevalence, severity, and nature of preventable patient harm across medical care settings: Systematic review and meta-analysis”, *bmj*, vol. 366, 2019.
- [26] “Spinal fusion - global analysis and market forecasts”, *GlobalData MediPoint*, 2014.
- [27] S. V. Kotsis and K. C. Chung, “Application of see one, do one, teach one concept in surgical training”, *Plastic and Reconstructive Surgery*, vol. 131, no. 5, p. 1194, 2013.

- [28] A. G. Gallagher *et al.*, “Virtual reality simulation for the operating room: Proficiency-based training as a paradigm shift in surgical skills training”, *Ann. of Surgery*, vol. 241, no. 2, p. 364, 2005.
- [29] C. E. Buckley, D. O. Kavanagh, O. Traynor, and P. C. Neary, “Is the skillset obtained in surgical simulation transferable to the operating theatre?”, *The Amer. J. of Surgery*, vol. 207, no. 1, pp. 146–157, 2014.
- [30] S. Alkadri *et al.*, “Utilizing a multilayer perceptron artificial neural network to assess a virtual reality surgical procedure”, *Comput. in Biol. and Med.*, vol. 136, p. 104770, 2021.
- [31] S. S. Y. Tan and S. K. Sarker, “Simulation in surgery: A review”, *Scottish medical journal*, vol. 56, no. 2, pp. 104–109, 2011.
- [32] I. Badash, K. Burt, C. A. Solorzano, and J. N. Carey, “Innovations in surgery simulation: A review of past, current and future techniques”, *Annals of translational medicine*, vol. 4, no. 23, 2016.
- [33] E. D. Grober *et al.*, “The educational impact of bench model fidelity on the acquisition of technical skill: The use of clinically relevant outcome measures”, *Annals of surgery*, vol. 240, no. 2, p. 374, 2004.
- [34] R. Michaels *et al.*, “3d printing in surgical simulation: Emphasized importance in the covid-19 pandemic era”, *Journal of 3D printing in medicine*, vol. 5, no. 1, pp. 5–9, 2021.
- [35] D. D. I. D. Service, *Global medic 15 [image 12 of 33]*, Date obtained: July 19, 2023, 2015. [Online]. Available: <https://www.dvidshub.net/image/2001366/global-medic-15>.
- [36] *File:a-experimental-design-b-first-person-view-and-c-automatic-performance-metrics-generated-by-the-voxel-man-tempo-surg-simul.jpg*, Date obtained: July 19, 2023. [Online]. Available: <https://commons.wikimedia.org/wiki/File:A-Experimental-design-b-first-person-view-and-c-automatic-performance-metrics-generated-by-the-Voxel-Man-TempoSurg-simul.jpg>.
- [37] D. J. Anastakis *et al.*, “Assessment of technical skills transfer from the bench training model to the human model”, *The American journal of surgery*, vol. 177, no. 2, pp. 167–170, 1999.
- [38] S. M. Werz, S. Zeichner, B.-I. Berg, H.-F. Zeilhofer, and F. Thieringer, “3d printed surgical simulation models as educational tool by maxillofacial surgeons”, *Eur J Dent Educ.*, vol. 22, no. 3, e500–e505, 2018.

- [39] J. R. Ryan, K. K. Almefty, P. Nakaji, and D. H. Frakes, “Cerebral aneurysm clipping surgery simulation using patient-specific 3d printing and silicone casting”, *World neurosurgery*, vol. 88, pp. 175–181, 2016.
- [40] C. L. Cheung, T. Looi, T. S. Lendvay, J. M. Drake, and W. A. Farhat, “Use of 3-dimensional printing technology and silicone modeling in surgical simulation: Development and face validation in pediatric laparoscopic pyeloplasty”, *J. Surg. Educ.*, vol. 71, no. 5, pp. 762–767, 2014.
- [41] P. Li, Z. Yang, and S. Jiang, “Tissue mimicking materials in image-guided needle-based interventions: A review”, *Mater. Sci. Eng. C*, vol. 93, pp. 1116–1131, 2018.
- [42] B. Stott and M. Driscoll, “Face and content validity of analog surgical instruments on a novel physics-driven minimally invasive spinal fusion surgical simulator”, *Med. & Bio. Eng. & Comput.*, vol. 60, no. 10, pp. 2771–2778, 2022.
- [43] K. Veluvolu and W. Ang, “Estimation and filtering of physiological tremor for real-time compensation in surgical robotics applications”, *The International Journal of Medical Robotics and Computer Assisted Surgery*, vol. 6, no. 3, pp. 334–342, 2010.
- [44] A. Zia, Y. Sharma, V. Bettadapura, E. L. Sarin, and I. Essa, “Video and accelerometer-based motion analysis for automated surgical skills assessment”, *International journal of computer assisted radiology and surgery*, vol. 13, pp. 443–455, 2018.
- [45] N. X. Anh, R. M. Nataraja, and S. Chauhan, “Towards near real-time assessment of surgical skills: A comparison of feature extraction techniques”, *Computer methods and programs in biomedicine*, vol. 187, p. 105 234, 2020.
- [46] S. L. Brunton and J. N. Kutz, *Data-driven science and engineering: Machine learning, dynamical systems, and control*. Cambridge University Press, 2022.
- [47] A. O. Frank, I. A. Twombly, T. J. Barth, and J. D. Smith, “Finite element methods for real-time haptic feedback of soft-tissue models in virtual reality simulators”, in *Proceedings IEEE Virtual Reality 2001*, IEEE, 2001, pp. 257–263.
- [48] P. Moreira, N. Zemiti, C. Liu, and P. Poignet, “Viscoelastic model based force control for soft tissue interaction and its application in physiological motion compensation”, *Comput. Methods and Programs in Biomedicine*, vol. 116, no. 2, pp. 52–67, 2014.
- [49] A. Wittek, G. Bourantas, B. F. Zwick, G. Joldes, L. Esteban, and K. Miller, “Mathematical modeling and computer simulation of needle insertion into soft tissue”, *PloS one*, vol. 15, no. 12, e0242704, 2020.
- [50] G. Ravali and M. Manivannan, “Haptic feedback in needle insertion modeling and simulation”, *IEEE reviews in biomedical engineering*, vol. 10, pp. 63–77, 2017.

- [51] M. Khadem, B. Fallahi, C. Rossa, R. S. Sloboda, N. Usmani, and M. Tavakoli, “A mechanics-based model for simulation and control of flexible needle insertion in soft tissue”, in *2015 IEEE Int. Conf. Robot. Automat. (ICRA)*, IEEE, 2015, pp. 2264–2269.
- [52] S. Misra, K. B. Reed, A. S. Douglas, K. Ramesh, and A. M. Okamura, “Needle-tissue interaction forces for bevel-tip steerable needles”, in *2008 2nd IEEE RAS & EMBS International Conference on Biomedical Robotics and Biomechatronics*, IEEE, 2008, pp. 224–231.
- [53] N. Abolhassani, R. Patel, and M. Moallem, “Needle insertion into soft tissue: A survey”, *Medical engineering & physics*, vol. 29, no. 4, pp. 413–431, 2007.
- [54] A. I. Aviles, S. M. Alsaleh, J. K. Hahn, and A. Casals, “Towards retrieving force feedback in robotic-assisted surgery: A supervised neuro-recurrent-vision approach”, *IEEE transactions on haptics*, vol. 10, no. 3, pp. 431–443, 2016.
- [55] Z. Pezzementi, D. Ursu, S. Misra, and A. M. Okamura, “Modeling realistic tool-tissue interactions with haptic feedback: A learning-based method”, in *2008 Symposium on Haptic Interfaces for Virtual Environment and Teleoperator Systems*, IEEE, 2008, pp. 209–215.
- [56] K. El-Monajjed and M. Driscoll, “Haptic integration of data-driven forces required to gain access using a probe for minimally invasive spine surgery via cadaveric-based experiments towards use in surgical simulators”, *J. of Comput. Sci.*, vol. 60, p. 101 569, 2022.
- [57] A. Pappalardo, A. Albakri, C. Liu, L. Bascetta, E. D. Momi, and P. Poignet, “Hunt–crossley model based force control for minimally invasive robotic surgery”, *Biomed. Signal Process. and Control*, vol. 29, pp. 31–43, Aug. 2016.
- [58] L. Barbé, B. Bayle, M. de Mathelin, and A. Gangi, “In vivo model estimation and haptic characterization of needle insertions”, *The Int. J. of Robot. Res.*, vol. 26, no. 11-12, pp. 1283–1301, 2007.
- [59] M. Ferro, C. Gaz, M. Anzidei, and M. Vendittelli, “Online needle-tissue interaction model identification for force feedback enhancement in robot-assisted interventional procedures”, *IEEE Trans. on Med. Robot. and Bionics*, vol. 3, no. 4, pp. 936–947, 2021.
- [60] L. Ljung *et al.*, “Theory for the user”, *System Identification*, 1987.
- [61] T. Hsia, *System Identification: Least-squares Method*. Lexington, MA: Lexington Books, 1978.
- [62] R. Fortune, *Fatigue structural testing enhancement research (FASTER)*. McGill University, 2020.

- [63] M. B. Tischler, *System identification methods for aircraft flight control development and validation*. Routledge, 2018.
- [64] D. T. Westwick and R. E. Kearney, *Identification of nonlinear physiological systems*. John Wiley & Sons, 2003, vol. 7.
- [65] M. Ayob, W. W. Zakaria, J. Jalani, N. M. Nasir, and M. M. Tomari, “Estimation of nonlinear arx model for soft tissue by wavenet and sigmoid estimators”, *Journal of Telecommunication, Electronic and Computer Engineering (JTEC)*, vol. 8, no. 7, pp. 123–128, 2016.
- [66] W. Edwards *et al.*, “Data-driven modelling and control for robot needle insertion in deep anterior lamellar keratoplasty”, *IEEE robotics and automation letters*, vol. 7, no. 2, pp. 1526–1533, 2022.
- [67] R. B. Graham and S. H. Brown, “A direct comparison of spine rotational stiffness and dynamic spine stability during repetitive lifting tasks”, *Journal of biomechanics*, vol. 45, no. 9, pp. 1593–1600, 2012.
- [68] N. P. Reeves, J. Cholewicki, J. H. Van Dieën, G. Kawchuk, and P. W. Hodges, “Are stability and instability relevant concepts for back pain?”, *journal of orthopaedic & sports physical therapy*, vol. 49, no. 6, pp. 415–424, 2019.
- [69] T. C. Franklin, K. P. Granata, M. L. Madigan, and S. L. Hendricks, “Linear time delay methods and stability analyses of the human spine. effects of neuromuscular reflex response”, *IEEE Transactions on Neural Systems and Rehabilitation Engineering*, vol. 16, no. 4, pp. 353–359, 2008.
- [70] A. D. Goodworth and R. J. Peterka, “Contribution of sensorimotor integration to spinal stabilization in humans”, *Journal of neurophysiology*, vol. 102, no. 1, pp. 496–512, 2009.
- [71] K. Granata, G. Slota, and B. Bennett, “Paraspinal muscle reflex dynamics”, *Journal of biomechanics*, vol. 37, no. 2, pp. 241–247, 2004.
- [72] M. M. Panjabi *et al.*, “The stabilizing system of the spine. part i. function, dysfunction, adaptation, and enhancement”, *Journal of spinal disorders*, vol. 5, pp. 383–383, 1992.
- [73] J. Cholewicki and S. M. McGill, “Mechanical stability of the in vivo lumbar spine: Implications for injury and chronic low back pain”, *Clinical biomechanics*, vol. 11, no. 1, pp. 1–15, 1996.
- [74] E. Maaswinkel, P. van Drunen, D.-J. H. Veeger, and J. H. van Dieën, “Effects of vision and lumbar posture on trunk neuromuscular control”, *Journal of biomechanics*, vol. 48, no. 2, pp. 298–303, 2015.

- [75] A. A. White III, R. M. Johnson, M. M. Panjabi, W. O. Southwick, *et al.*, “Biomechanical analysis of clinical stability in the cervical spine”, *Clinical Orthopaedics and Related Research®*, vol. 109, pp. 85–96, 1975.
- [76] W. Kirkaldy-Willis, “Presidential symposium on instability of the lumbar spine: Introduction”, *Spine*, vol. 10, no. 3, p. 254, 1985.
- [77] N. P. Reeves, K. S. Narendra, and J. Cholewicki, “Spine stability: The six blind men and the elephant”, *Clinical biomechanics*, vol. 22, no. 3, pp. 266–274, 2007.
- [78] H. K. Khalil, *Nonlinear systems*. Prentice Hall, 2002.
- [79] K. P. Granata and S. A. England, “Stability of dynamic trunk movement”, *Spine*, vol. 31, no. 10, E271, 2006.
- [80] S. McGill and R. W. Norman, “Reassessment of the role of intra-abdominal pressure in spinal compression”, *Ergonomics*, vol. 30, no. 11, pp. 1565–1588, 1987.
- [81] C. Larivière, D. Ludvig, R. Kearney, H. Mecheri, J.-M. Caron, and R. Preuss, “Identification of intrinsic and reflexive contributions to low-back stiffness: Medium-term reliability and construct validity”, *Journal of biomechanics*, vol. 48, no. 2, pp. 254–261, 2015.
- [82] M. T. Rosenstein, J. J. Collins, and C. J. De Luca, “A practical method for calculating largest lyapunov exponents from small data sets”, *Physica D: Nonlinear Phenomena*, vol. 65, no. 1-2, pp. 117–134, 1993.
- [83] K. Granata and P. Gottipati, “Fatigue influences the dynamic stability of the torso”, *Ergonomics*, vol. 51, no. 8, pp. 1258–1271, 2008.
- [84] R. B. Graham, E. M. Sadler, and J. M. Stevenson, “Does the personal lift-assist device affect the local dynamic stability of the spine during lifting?”, *Journal of biomechanics*, vol. 44, no. 3, pp. 461–466, 2011.
- [85] P. A. Parrilo, *Structured semidefinite programs and semialgebraic geometry methods in robustness and optimization*. California Institute of Technology, 2000.
- [86] A. Ahmadi, *Sum of squares (sos) techniques: An introduction*. [Online]. Available: https://www.princeton.edu/~aaa/Public/Teaching/ORF523/S16/ORF523_S16_Lec15.pdf.
- [87] S. Shen and R. Tedrake, “Sampling quotient-ring sum-of-squares programs for scalable verification of nonlinear systems”, in *2020 59th IEEE Conference on Decision and Control (CDC)*, IEEE, 2020, pp. 2535–2542.
- [88] R. Tedrake, *Underactuated Robotics, Algorithms for Walking, Running, Swimming, Flying, and Manipulation*. 2023. [Online]. Available: <https://underactuated.csail.mit.edu>.

- [89] R. Tedrake, I. R. Manchester, M. Tobenkin, and J. W. Roberts, “Lqr-trees: Feedback motion planning via sums-of-squares verification”, *The International Journal of Robotics Research*, vol. 29, no. 8, pp. 1038–1052, 2010.
- [90] A. Majumdar and R. Tedrake, “Funnel libraries for real-time robust feedback motion planning”, *The International Journal of Robotics Research*, vol. 36, no. 8, pp. 947–982, 2017.
- [91] M. M. Tobenkin, I. R. Manchester, and R. Tedrake, “Invariant funnels around trajectories using sum-of-squares programming”, *IFAC Proceedings Volumes*, vol. 44, no. 1, pp. 9218–9223, 2011.
- [92] A. Majumdar, A. A. Ahmadi, and R. Tedrake, “Control design along trajectories with sums of squares programming”, in *2013 IEEE International Conference on Robotics and Automation*, IEEE, 2013, pp. 4054–4061.
- [93] P. D. Holmes, S. M. Danforth, X.-Y. Fu, T. Y. Moore, and R. Vasudevan, “Characterizing the limits of human stability during motion: Perturbative experiment validates a model-based approach for the sit-to-stand task”, *Royal Society open science*, vol. 7, no. 1, p. 191 410, 2020.
- [94] V. Shia, T. Y. Moore, P. Holmes, R. Bajcsy, and R. Vasudevan, “Stability basin estimates fall risk from observed kinematics, demonstrated on the sit-to-stand task”, *Journal of biomechanics*, vol. 72, pp. 37–45, 2018.
- [95] N. P. Reeves, J. Cholewicki, and K. S. Narendra, “Effects of reflex delays on postural control during unstable seated balance”, *Journal of biomechanics*, vol. 42, no. 2, pp. 164–170, 2009.
- [96] Y. Xu, J. Choi, N. P. Reeves, and J. Cholewicki, “Optimal control of the spine system”, 2010.
- [97] H. K. Kim, D. W. Rattner, and M. A. Srinivasan, “Virtual-reality-based laparoscopic surgical training: The role of simulation fidelity in haptic feedback”, *Comput. Aided Surgery*, vol. 9, no. 5, pp. 227–234, 2004.
- [98] M Capurro, F Barberis, P Dubruel, and S Van Vlierberghe, *Biomaterials for bone regeneration*, 2014.
- [99] T. Cotter, R. Mongrain, and M. Driscoll, “Vacuum curette lumbar discectomy mechanics for use in spine surgical training simulators”, *Scientific Reports*, vol. 12, no. 1, p. 13 517, 2022.
- [100] R. Haddas and I. H. Lieberman, “A method to quantify the “cone of economy””, *European Spine Journal*, vol. 27, pp. 1178–1187, 2018.

- [101] K. Hasegawa and J. F. Dubousset, “Cone of economy with the chain of balance-historical perspective and proof of concept”, *Spine Surgery and Related Research*, vol. 6, no. 4, pp. 337–349, 2022.